Recent Advances in Molecular Simulations of Ion Solvation at Liquid Interfaces

Tsun-Mei Chang

Department of Chemistry, University of Wisconsin—Parkside, 900 Wood Road, Box 2000, Kenosha, Wisconsin 53141

Liem X. Dang*

Chemical Sciences Division, Pacific Northwest National Laboratory, Richland, Washington 99352

Received August 6, 2005

Contents

1. Introduction and Scope

The solvation and adsorption of ions at the aqueous interfaces is an important process encountered in numerous chemical and biological systems.[1−4] The influence of ions on the liquid interfaces is not only of fundamental interest but also of practical significance. For example, the transfer mechanisms and free energies of ions across liquid surfaces are essential to solvent extraction processes and phase transfer catalysis.[5] The stability and functionality of cell membranes will be affected by the distribution of counterions. Understanding ion behavior at the air/water interface is crucial in solving environmental problems such as acid rain and water pollution.[6] In atmospheric chemistry studies, the uptake of pollutants by water clouds depends on the ion distribution at the aqueous liquid/vapor interface. Understanding the equilibrium properties and dynamics of ions at a wide range of liquid interfaces is essential in modeling and controlling the chemical reactivity at liquid interfaces.

Many-body effects in the hydrogen-bonded network have been studied in detail and, in particular, through the evaluation of changes in the molecular dipole moment as a function of its environment. Substantial efforts have been undertaken to quantify the many-body effects using different approaches, such as classical dynamics and *ab initio* simulations. The dipole moment of an isolated water molecule is 1.85 D, and because of induction effects, it significantly increases upon addition of water molecules in a cluster and the condensed phase. The computed average dipole moments of water molecules near the interface are relaxed to their gas-phase values because of changes in the electric field, while water molecules farther from the interface have dipole moments that correspond to their bulk values.

Despite the fundamental importance of liquid surfaces, characterization of these interfaces at the molecular level is rather limited both theoretically and experimentally. Past experimental studies on liquid interfaces mostly relied on thermodynamic measurements such as surface tension or surface potential to infer the microscopic structures at the interfaces. Other surface-specific techniques either are not suitable for vapor/liquid interface studies (because of the vapor pressure) or are restricted by the underlying physical models. Advances in modern instrumentation have significantly improved this situation. Experimental techniques such as nonlinear-optical spectroscopy (second harmonic generations or sum frequency generations), X-ray diffraction and reflection, and neutron reflection, which are capable of measuring molecular details at the interface, have been recently developed.[7−13] Among these approaches, nonlinear optical methods have made the major contributions to our understanding of interfaces. This technique has been successfully applied to investigate the structure of surface-active solutes and the surfaces of pure liquids. In the past few years, this method has been extended to examine the behavior of ions at liquid/vapor interfaces.[14−16]

Molecular simulation approaches such as molecular dynamics (MD) and Monte Carlo (MC) techniques provide other useful tools to study liquid interfaces.[17] They have the advantage over experiments in that they can directly probe the molecular details of solutes at the interface. Since the late 1980s, molecular simulations have been widely used to examine the equilibrium properties of neat liquid/vapor and liquid/liquid interfaces.[18−23] Results from these studies have provided valuable information on the structures, thermodynamics, dynamics, and conformational equilibriums of liquid interfaces. These approaches have subsequently been used to study the ion solvation and ion transport across the liquid/vapor interfaces, revealing new insights into ion behavior at liquid interfaces.

10.1021/cr0403640 CCC: $59.00
Published on Web 12/14/2005

Tsun-Mei Chang obtained her B.S. degree in Chemistry from National Taiwan University in Taipei, Taiwan. She received her Ph.D. degree in Chemical Physics from Columbia University in the city of New York, under the direction of Professor James L. Skinner. Her thesis work was on the applications of statistical mechanics to condensed phase phenomena and spectroscopy. She held a postdoctoral position at the University of California—Los Angeles, studying solid thin film morphology. As an AWU Postdoctoral Fellow at Pacific Northwest National Laboratory, she worked on molecular simulations of liquids. She was also a visiting scholar at the University of Illinois—Urbana-Champaign, where she studied phase behavior of polymer blends. In 1999, she joined the faculty at the University of Wisconsin—Parkside, where she is currently an Associate Professor of Chemistry. Chang's research interests include the theoretical and computational studies of structures and dynamics in complex fluid systems.

Liem X. Dang was born in Hue, Vietnam. He and his older brother imigrated to the U.S. in 1975. Liem X. Dang received his B.S. with Honors in Chemistry with a minor in Mathematics in 1980 from Florida Institute of Technology and his Ph.D. in Physical Chemistry in 1985 from the University of California—Irvine, under the guidance of Professor Max Wolfsberg. He had worked with Monte Pettitt of University of Houston and with the late Peter Kollman of UCSF. He is currently a Chief Scientist at the Pacific Northwest National Laboratory. He has authored or coauthored over 80 peer-reviewed publications on the development and use of molecular dynamics computer simulation techniques to study molecular complex systems.

One essential question about solvation at an interface regards the details of ion distributions.[24] The traditional view of interfaces being devoid of ions comes from surface tension measurements.[25−29] It has been long recognized that small inorganic ions in aqueous solutions alter the surface tension. In general, simple inorganic salts, such as NaF and LiCl, increase the surface tension of aqueous solutions. The increment is roughly linear with the salt concentration. The increase in surface tension by the addition of simple salts has been explained as repulsion or negative adsorption of ions from the liquid/vapor interface in which the ion concentration is lower than that of the bulk solution. This interpretation is based on the Gibbs adsorption isotherm[30,31]

$$\Gamma = -\frac{1}{RT}\left(\frac{\mathrm{d}\gamma}{\mathrm{d}\ln a}\right)_T \quad (1)$$

In the above equation, Γ is the surface excess concentration of the solute (ion), R is the ideal gas constant, T is the temperature, and γ is the surface tension. When applying this equation, the Gibbs dividing surface (GDS) is chosen such that the surface excess of solvent is zero. Here, a is the activity of the ion. In dilute solutions, a is proportional to the concentration. Thus, if the surface tension increases linearly with the concentration, there is a deficiency of the solutes in the surface layer.[32] The theory of surface tension change with added salt concentrations was first qualitatively explained by Wagner based on the Debye−Huckel theory of electrolytes.[33] He argued that, because of the variation in the dielectric constants across the interface, the presence of ions at the interface induces image surface charges that have the same magnitude and sign. The image charges repel the ions from the surface and thus reduce the concentrations of ions at the interface. The surface tension accordingly increases on addition of a simple electrolyte. Onsager and Samaras further worked out the theory and obtained an analytical limiting law of the salt effect on surface tension.[34] Recently, other theoretical approaches, including field theoretical calculations and canonical thermodynamic theory, have been developed to explain the effect of electrolyte concentrations on the surface tension.[35−38] These theories recover the Onsager−Samaras limiting law and revealed negative adsorption of ions at the interface.

This conventional view of the surface being free of ions has been challenged in the past few years by both simulation and experimental work. In the studies of atmospheric reactions on aqueous sea salt particles and ocean surfaces, the most plausible reaction mechanisms involve the presence of ions at the surface.[39−41] This finding motivated other[42,43] theoretical and experimental[44] studies to investigate the possible presence of ions at liquid/vapor interfaces. Molecular dynamic simulations using polarizable potentials showed[45] that while the small nonpolarizable cations and anions including Na^+ and F^- are repelled from the interface, larger polarizable anions such as Cl^- and Br^- ions are found to be surface active and exhibit an enhancement in their surface concentrations. This conclusion is also reached by the results of second harmonic generation (SHG) or sum frequency generation (SFG) experiments on the surfaces of aqueous salt solutions as well as the surfaces of aqueous acids and bases.[44,46] It should be noted that the affinity of ions at the interfaces is not necessary in violation of Gibbs adsorption isotherm. The thermodynamic argument only requires the total ion concentration in the interfacial region to be depleted and does not provide a detailed molecular description of the interfacial ion distribution along the surface normal direction. Thus, it is possible to have nonmonotonic ion density profiles such that the total concentration in the interfacial region is less than that of the bulk. This nonuniform ion distribution has been observed in simulations and will be discussed further in the following sections.

Our knowledge of liquid/liquid interfaces has advanced a great deal due to computer simulation studies. Since the late 1980s, several research groups have used MC and MD simulations to investigate the equilibrium properties of neat liquid/liquid interfaces. The results reported by these groups[47,48] have provided valuable insight into the structures, dynamics,

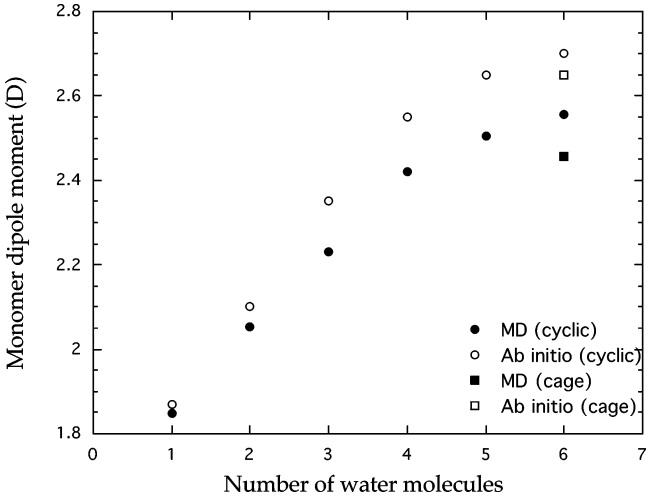

Figure 1. Computed average dipole moment/water molecule as a function of cluster size. The MD data are from ref 52 while the *ab initio* results are from ref 50. The cyclic water hexamer is also called the ring structure formed by six water molecules in which each water molecule is hydrogen bonded to the two nearest water molecules. In addition, four oxygen atoms are lying on the same plane, and the remaining oxygen atoms lie on either side of this plane. The cage structure is held together by eight hydrogen bonds. This is a three-dimensional structure network in which four water molecules are hydrogen bonded together and the remaining two water molecules lie on the top and bottom of these doubly hydrogen-bonded water molecules to form a cagelike structure.

thermodynamics, and conformational equilibria of liquid interfaces. This approach has been extended to study the transport free energies of ions and organic solutes across liquid/liquid interfaces.[48,49] The use of these simulation techniques provides a means to directly probe the mechanisms and dynamics of transport processes of small organic solutes and ions across liquid/liquid interfaces.

In this paper, we present a review of the application of MD simulation methods, ranging from polarizable potential models used to describe interactions among species to a variety of chemical and physical processes in solutions and at interfaces from the late 1980s to the present. The main emphasis of the review is on recent advances in the understanding of ion solvation, molecular association, and molecular solvation at liquid interfaces. The species discussed range from monovalent ions to molecular ions such as hydronium and nitrate ions. The computed properties include the potential of mean force, the surface tension, the surface potential, and the density profile. Comparisons with experimental results were made and are discussed in the review.

2. Significance of Polarizable Potential Models

It is well established that nonadditive interactions are a significant contributor to the total interaction energy. The incorporation of many-body interactions into potential models is especially critical for the study of clusters and interfacial environments. For example, it is well established that the dipole moment of an isolated water molecule is 1.85 D, and because of induction effects, the average dipole moment/water molecule in clusters significantly increases upon addition of water molecules. In Figure 1, a comparison between the computed average dipole moment reported by Gregory and co-workers[50] using quantum chemical methods and the results by Dang and Chang using a classical water model that explicitly includes many-body effects is made.[51,52]

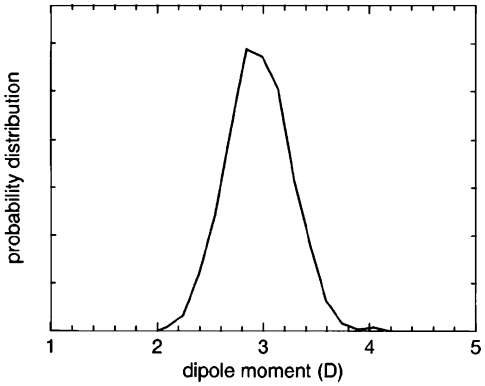

Figure 2. Distribution of the modulus of the water molecule dipole moment in liquid water obtained using 12 MD configurations. The unit of the *y*-axis is arbitrary. (Adapted from ref 53.)

Considering the difference in computational methods, the agreement between the two approaches is quite satisfactory. A reasonable conclusion from this comparison is that the major differences in the two calculations are caused by the differences in the dipole moment of the isolated water monomer ($\mu = 1.848$ D for the potential model vs 1.869 D for the *ab initio* calculation) and the fact that no explicit charge-transfer term is included in the MD model. This comparison illustrates the importance of polarization effects in water clusters and demonstrates that the structure and properties of water clusters can be accurately reproduced only if the polarizability is accounted for explicitly in the potential model.

There is a significant effort using both computational[53] and experimental[54] approaches to determine the molecular dipole moment of a water molecule in the liquid phase. Silvestrelli and Parrinello reported an *ab initio* MD study to determine the change that the electric dipole moment of water molecules undergoes in passing from the gas to the liquid phase.[53] Their analyses were based on the recently introduced maximally localized Wannier functions. They found that, in the liquid water, the dipole moment has an average value of about 3 D, which is 60% higher than that in the gas phase. Furthermore, a broad distribution around this average value is observed as shown in Figure 2. Badyal el al.[54] have reported a first experimental high-energy, X-ray measurement estimate of the dipole moment of liquid water. Their value for the dipole moment of the H_2O molecule is 2.96 ± 0.6 D, which is based on a charge transfer of 0.5*e* along each O−H bond, with an experimental uncertainty of order 20%. This value agrees with theoretical estimates published in the literature. *Ab initio* cluster calculations yielded a dipole moment value of 2.7 D. Classical MD simulations by Dang and Chang[51] derived permanent and induced dipole moments of 0.94 and 1.85 D, giving a total dipole moment of 2.75 D, while recent *ab initio* molecular dynamics simulations yielded a dipole moment of 2.95 D. Within the stated uncertainty, the measurements of Badyal and co-workers represent the first experimental estimate of the dipole moment of liquid water, a quantity that plays a crucial role in determining the dielectric properties of the liquid.

Batista and co-workers[55] used a self-consistent induction model to study the electric field in ice and found that the best estimate for the dipole moment of a water molecule in ice *Ih* is 3.09 D. This value represents a 67% increase over the dipole moment of an isolated water molecule. The result is shown in Figure 3. The dipole moment determined by Batista et al. is significantly higher than the one reported

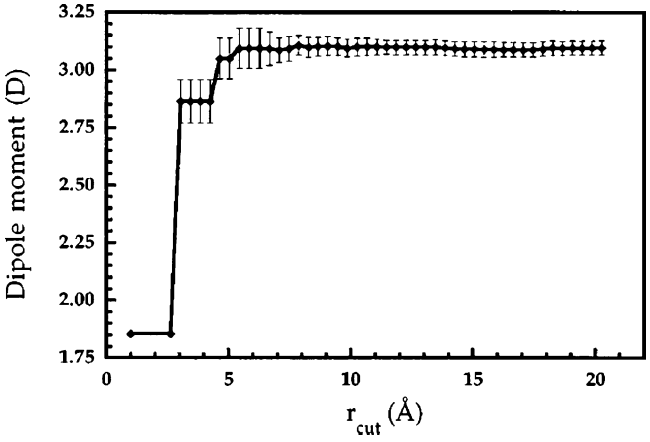

Figure 3. Convergence of the calculated molecular dipole moment as a function of the cutoff distance used in summing the electric potential caused by neighbors. The error bars correspond to the fluctuations caused by the different environments seen by the various molecules in the proton disordered ice *Ih*. The results show that it is sufficient to include only neighbors that are closer than 7 Å when evaluating the electric field at a given molecule. (Adapted from ref 55.)

earlier by Coulson and Eisenberg,[56] who also used a similar but more approximate induction model. The difference between the results of Batista and co-workers and the earlier estimates mainly lies in the numerical values for the quadrupole moment of the isolated molecule. Coulson and Eisenberg relied on the best estimates of multipole moments from first-principle calculations at the time, which included a very small basis set. Batista and co-workers used experimental values for the dipole and quadrupole moments,[57,58] the latter obtained after Coulson and Eisenberg carried out their calculation, and the results of accurate *ab initio* calculations for the higher octopole and hexadecapole moments. When the same set of multipoles are used as input, the method used by Coulson and Eisenberg gave results that are very similar to those obtained by the more detailed model used by Batista and co-workers. This similarity of results indicates that the approximations used by Coulson and Eisenberg to simplify the induction calculations are quite valid.

It is widely accepted that water molecules behave differently at the interface than in bulk solution. The advantage of using polarizable potentials is that they can describe the electrostatic properties of water molecules in heterogeneous environments more realistically. To study the effects of polarization on the electrical properties of the water molecules, Dang and Chang[51] computed the average total dipole moment and the induced dipole moment/water molecule as a function of position along the *z*-axis. The result is shown in Figure 4. Examining this figure, they observed that the water molecules farther from the interface (in the regions between 30 and 45 Å) have an average dipole moment of 2.75 D and an average induced dipole moment of 0.93 D. These values are very close to the values obtained for simulations of bulk solutions. On the other hand, the water molecules residing in the vicinity of the interface have completely different average dipole moment values. Figures 4 and 5 clearly indicate that the average dipole moments of water molecules monotonically decrease as they approach the interface and reach a value close to their gas-phase dipole moment. Dang and Chang found that the corresponding average induced dipole moments also become smaller. These results are expected and are physically realistic. They are

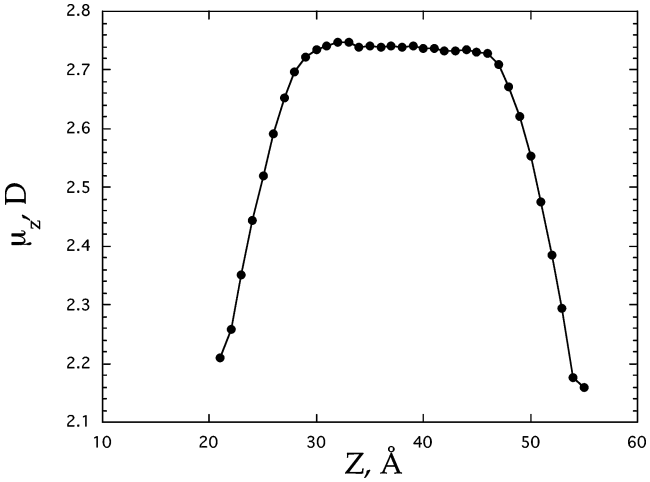

Figure 4. Computed dipole moment of water molecules as a function of the *z*-coordinate using classical molecular dynamics techniques. (Adapted from ref 51.)

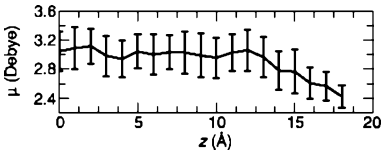

Figure 5. Computed dipole moment of water molecules as a function of the *z*-coordinate using *ab initio* molecular dynamics techniques. (Adapted from ref 59.)

caused, in part, by changes in the hydrogen-bonding patterns (i.e., the number of hydrogen bonds per water molecule in bulk is about 4, and the number is decreased to about 2 for water molecules near the interface) and also by changes in the electric field of water molecules near the interface. Recently, Kuo and Mundy[59] reported an *ab initio* MD study of the aqueous liquid/vapor interface. In addition to the computed structural and spectra properies of the interface, they also computed the dipole moment of water molecules as a function of the *z*-axis. Their results, which are shown in Figure 5, are similar to those reported by Dang and Chang.

3. Computational Results of Liquid Water Interfaces

3.1. Ion Distribution at Interfaces

Some of the most interesting and outstanding questions about ion solvation at liquid interfaces involve the distribution of the ions: (a) Where does the ion spend most of the time? (b) Are ions surface active and staying near the interface, or do they prefer to be fully immersed in the bulk liquids?

3.1.1. Distribution of Ions in the Gas Phase

Understanding such behavior will significantly advance our understanding of the chemical reactivity of ions at liquid interfaces. Early hints that some ions may be surface active at liquid/vapor interfaces come from a series of MD simulations of ion−water clusters by Berkowitz and co-workers to study the solvation behavior of Na^+ and Cl^- ions in small water clusters.[60−64] In these studies, two kinds of potential models—one an effective pairwise additive model and the other a nonadditive many-body potential model—were used to understand the polarization effects. Berkowitz and co-workers found that potential model and ion charge

had a significant affect on the structure and stability of ionic water clusters. For the $Na^+(H_2O)_6$ cluster, the polarization potential model predicted a first hydration shell made of four water molecules while the nonpolarizable model predicted a six-water solvation shell. The effect is more pronounced for anions. With the polarizable model, the Cl^- ion was found to locate on the surface of the cluster while the Cl^- ion was completely solvated by water when effective pair potential was used. On the other hand, they found that a small halide anion F^- remained solvated inside the water cluster. Dang and co-workers[65] and Dang[66] used many-body polarizable potential models in MD simulations to study the solvation behavior of Li^+, Na^+, Cl^-, and F^- ions in water clusters. They observed that both F^- and Cl^- ions preferred to remain at the surface of the water cluster.

At the same time, novel experimental techniques have been developed to examine the ion solvation and hydrogen bonding in small water clusters.[67−74] These experiments revealed that the larger halide ions such as Cl^-, Br^-, and I^- were solvated asymmetrically in water clusters of up to six water molecules. These findings suggested that larger halide ions were solvated on the surface of water clusters, which agreed with the simulation results.

These observations have led to continuous interest in the study of ion hydration in water clusters.[75−82] *Ab inito* calculations have been carried out to examine the optimized structure of aqueous ionic clusters.[83−86] These quantum studies also showed that, in small aqueous clusters, larger halide anions preferred the surface state over the interior state as the global minimum, while F^- ion favored the interior state. Although it is established that Cl^-, Br^-, and I^- ions prefer to locate at the surface of smaller aqueous clusters, it is less obvious whether the ions would have the tendency to stay at the bulk liquid/vapor interface. Arguments have been made that, in addition to the polarizability of ions, the surface curvature of the clusters also plays an important role in determining the solvation behavior of ions.[78] It is generally accepted that ions remain fully solvated at the planar liquid surface. This conclusion is supported by experimental results on surface tension and surface potential measurements.[87]

3.1.2. Distribution of Ions in the Condensed Phase

The first MD simulation on ion solvation at the water liquid/vapor interface was carried out by Wilson et al.[88] They studied the behavior of the Na^+ ion at the interface and found that, not surprisingly, Na^+ ions remain completely solvated inside the water. They also compared their results to the prediction of a simple dielectric model and found that the dielectric model does not describe the simulation results satisfactorily. In a subsequent paper,[89] they extended the study to the study of the Na^+, F^-, and Cl^- ions near the water liquid/vapor interface. Using the umbrella sampling technique along the interfacial normal direction, they were able to compute the solvation free energy profiles of the ions as a function of their distance to the interface. They showed that the free energies of moving an ion to the interface depended on the sign of the ionic charge and not on the size of the ion. In all three cases, the free energy was observed to increase near the interface region, suggesting that ions preferred to be solvated in the bulk liquid region. Benjamin also carried out an MD simulation to investigate ion solvation at the water liquid/vapor interface.[90] He observed that ions tend to keep most of their first solvation shell intact and have positive adsorption free energies when they are moved to the interface. This finding indicates a negative adsorption of ions in the interfacial region. These studies seemed to confirm the classical picture of electrolyte solutions in which ions are negatively adsorbed at the water/air interface. In all the studies mentioned above, nonpolarizable interaction potential models were employed to describe the water−water and ion−water interactions.

Recently, Finlayson-Pitts and co-workers conducted a combination of experimental, MD, and kinetic modeling studies to examine the interfacial properties of aqueous NaCl aerosols.[39] The experimentally observed production of Cl_2 gas can only be explained by interfacial reactions (i.e., the aerosols' interfacial regions), which suggests a large presence of the ions at the interface. To confirm this result, a series of MD simulations were carried out on concentrated NaCl aqueous systems that range from water clusters to an infinite open liquid/vapor interface. Both polarizable and nonpolarizable models are employed to describe the molecular interactions. These simulations predicted that Na^+ ions are fully solvated and almost exclusively located in the interior of the liquid phase. On the other hand, both models found that Cl^- ions spend a significant amount of time near the interface. Quantitatively, the polarizable model predicted a much higher percentage of surface coverage of Cl^- ions than that of the nonpolarizable model. This finding seems to contradict the traditional wisdom that ions in salt solutions are negatively adsorbed at the interface.

This work has motivated a renewed interest in advancing the understanding the behavior of ions at the liquid/air interface through the use of both experimental[44,46,91−95] and theoretical approaches.[42,43,45,96−98] Jungwirth and Tobias carried out a series of detailed MD simulations to study the liquid/vapor interface of salt solutions.[43,91,96,99−102] They examined the behavior of aqueous acid, base, and salt solutions containing Na^+, F^-, Cl^-, Br^-, and I^- ions. In addition to monatomic ions, they also examined molecular ions including OH^-, H_3O^+, SO_4^{2-}, NO_3^-, and SCN^-. Only polarizable potential models were used in these studies because they have been shown necessary to properly describe the aqueous ionic clusters.[64] In the simulations, they observed diminished concentrations of small ions such as F^-, Na^+, and OH^- at the interface. This finding suggested that these ions are repelled from the interface, which agrees with the traditional description. However, when the density profiles of H_3O^+, NO_3^-, Cl^-, Br^-, and I^- are examined, they exhibit a peak near the interface. From these results, they concluded that these ions penetrated into the vapor/solution interface and had higher concentrations at the surface than that of the bulk solutions. The peak became increasingly more prominent as the halide anion got larger and more polarizable, which suggested that larger halide ions such as Br^- or I^- displayed more pronounced surface enhancement than Cl^- anion. Interestingly, when the density profiles of I^- from simulations of 1.0 M HI and NaI aqueous solutions are compared, an increase and shift in the interfacial density peak is observed for the acid. Because both H_3O^+ and I^- ions are surface active, their mutual attraction may further enhance the ions' presence at the interface. From the series of MD studies, Jungwirth and co-workers concluded that molecular polarizability played a key role in the surface affinity of ions, with higher polarizability leading to stronger surface enhancement. The only exception is the highly polarizable sulfate ion, SO_4^{2-}, which was found to show negative adsorption at the interface. This behavior was attributed to

the large energy penalty associated with surface solvation of SO_4^{2-} because of the double charge of sulfate anion.

Using the multistate empirical valence bond (MS-EVB) methodology, Voth and co-workers performed MD simulation to examine the hydrated proton at the water liquid/vapor interface.[103] The MS-EVB model provided a more physically realistic description of proton behavior by allowing the proton to hop along an optimal conformation of water molecules based on the Grotthuss mechanism.[104] The computed density profile in their work exhibited a significant peak at the interface and demonstrated that the hydrated excess proton displays a marked preference for the liquid/vapor interface.

There are many experimental results supporting the conclusion that some ions may be preferentially adsorbed at the water/air interface.[44,46,91−93,105] Advances in nonlinear optics techniques such SHG or SFG have made it possible to specifically probe molecules and ions at the interface.[9,10,106−108] For example, using femtosecond SHG experiments to exploit the charge-transfer-to-solvent (CTTS) resonance of several ions, Saykally and co-workers were able to measure directly the ion concentration at the surface of the aqueous solutions.[93,105,109] By examining the intensity of the SHG response to the CTTS transition, Saykally and co-workers directly probed the surface concentration of the anion as a function of the bulk salt concentration. They found an enhancement of the surface concentration of the highly polarizable anions such as N_3^-, SCN^-, and H_3O^+, which agrees with the predications from MD simulations.

Using vibrational SFG spectroscopy, Allen and co-workers examined the interfacial water structures for the sodium halide aqueous solutions.[44] The surface SFG spectra for the solutions of NaF and NaCl are similar to that of neat water; they concluded that similar interfacial water structures exist for the NaF and NaCl aqueous solutions compared to those for the neat water/vapor interface. A significant difference is observed for the SFG spectra of NaBr and NaI solutions compared to that of neat water, revealing a considerable distortion of the hydrogen-bonding network in the interfacial water of the sodium bromide and iodide aqueous solutions. The interfacial region is further affected as the concentration of the larger and more polarizable halogen anions is increased. Their results may imply higher concentrations of bromide and iodide anions in the interfacial region.

Richmond and co-workers also used a vibrational sum frequency spectroscopic technique to investigate the molecular structures and bonding of the surface of aqueous salt solutions of NaF, NaCl, NaBr, and NaI.[46] They observed a modification in the interfacial hydrogen bonding as the anion is changed, which may suggest the presence of anions near the interface. When the water structure of the topmost surface layer is examined, the perturbation caused by the anions becomes smaller, indicating a diminished population of the anions at the uppermost surface water layer. We note here that the somewhat different conclusions reached by these two groups interpreting practically the same data indicate that further research is required to systematically assign the characteristics in the hydrogen-bonded OH region of the VSFG (vibrational sum frequency generation) spectrum of aqueous salt solutions.

Using X-ray photoelectron spectroscopy,[92] Hemminger and co-workers measured the composition in the surface region of the potassium bromide and potassium iodide solutions. From the photoemission spectra, they were able to determine the anion/cation atomic ratio as a function of the photoelectron kinetic energy. Both KI and KBr showed significant enhancement of the halide ion concentration in the more surface-sensitive experiments. The enrichment of anion concentration is more dramatic for the larger, more polarizable iodide anion.

From what has been reported so far, it appears that larger polarizable anions are surface active at the water/vapor interface. However, this picture conflicts with the classical view that, based on the surface tension measurement and the Gibbs adsorption isotherm, the interface of a salt solution is devoid of ions. What is the reason for the enhancement of ion concentration at the liquid/vapor interface? Why does it happen more readily for larger and more polarizable ions than for the smaller nonpolarizable ions? To understand the behavior of ions at the interfaces, several factors must be considered. First, from a molecular interaction consideration, ions may be expected to be repelled from the interfacial region, in which the strong ion−water hydration energy will be missing because of the decreasing number of water molecules. To maintain the solvation shell, ions prefer to be fully immersed in the bulk solution phase. However, the ion effect on the water interaction also needs to be taken into account. According to the relative abilities of ions to induce the structuring of water molecules, ions have long been classified as being either kosmotropes (structure makers) or chaotropes (structure breakers).[110,111] If an ion tends to strongly order the water structure around it and break the hydrogen bonding between water, it is expected that this type of ions will be more prone to stay near the surface. In contrast, if an ion does not disturb the hydrogen bonding of the neighboring water, the tendency for the ion to stay in the interior of the bulk liquid becomes more significant.

The second factor is the effect of ion polarizability, which has been recognized to have a significant affect on the behavior of ion solvation.[80,112] Because of the presence of the liquid/vapor interface, water molecules at the interface show a preferred orientation.[10,113,114] This orientational order induces an electrostatic potential difference between the liquid and vapor phases. Small nonpolarizable ions were repelled from the interface because they are unable to respond to the electric field change. For ions with larger polarizabilities, the electron clouds of these ions can be more easily distorted to react with the interfacial electric field, leading to a favorable adsorption of these ions at the interfaces. As expected, this tendency will be enhanced with increasing ion polarizability, as predicted by the simulations and confirmed by the experiments. The only exception in the above studies is the sulfate ion. Despite its high polarizability, sulfate ions are found to be strongly repelled from the surface. This behavior results from the large electrostatic penalty and strong perturbation to the hydrogen-bonding network of interfacial water by bringing sulfate ions into the interface.

Conclusions obtained from surface tension measurements of salt solutions must be addressed. As the concentration of salt increases, the surface tension of the solution also increases. On the basis of the Gibbs adsorption isotherm of surface tension, the surface tension increment with added electrolyte concentration corresponds to negative adsorption of ions at the interface. Thus, the current view of the affinity of large halide anions and other ions at the water surface seems to be inconsistent with this prediction. However, it should be realized that the propensity of ions to accumulate at an interface does not necessarily lead to positive adsorption of ions if the possibility of nonuniform density profiles of

the ions is included. If we more closely examine the density profiles obtained from simulations, we note a decrease in the ion density toward the bulk phase after an initial density peak is observed at the interface. The combined effect of surface enhancement and the subsequent depletion of ion density may lead to a net negative excess of ion concentrations at the interfacial region. Thus, surface enhancement of certain ions does not necessarily violate Gibbs adsorption equations.

Studies are now being extended to investigate ion solvation at other nonaqueous solution interfaces.[115] Dang carried out an MD study to examine the behavior and equilibrium properties of sodium iodide at the liquid/vapor interface of methanol. He found that iodide anions penetrated more deeply into the interfacial region than sodium cations. However, no interfacial peak was observed in the density profile of iodide ions in methanol solution. This result is quantitatively different from that at an aqueous solution interface and indicates that the iodide ion does not show surface affinity for the methanol liquid/vapor interface. This behavior may be caused by the presence of an apolar methyl group in methanol molecules.

Other properties that play important roles in the reactivity of chemical species at interfaces are their orientations and local structures. To describe interfacial structure, the pair correlation distribution functions and angular distribution functions are generally analyzed. Both experimental and theoretical work have shown that surfaces significantly affect molecular orientation at interfaces.[15,18,90,113,116−119] In the bulk liquid region, because of the high symmetry, no specific orientational order is expected. As molecules move to the interfacial region, there is an increasing tendency to align themselves because of the electrostatic potential difference between the liquid and vapor phases. In aqueous solutions, there also is strong directional bonding between water molecules. These combined factors affect not only the orientation of water molecules but also the orientation between ions and water molecules. To provide a microscopic description of the molecular orientation, we analyze the behavior of angular distribution functions, which depicts the probability distribution of the angle between some chosen molecular axis and the surface normal direction. These functions will provide a direct measure of the molecular orientation at the interface. In a study of ion solvation at the water interface, Benjamin discussed the probability distribution function of the angle between the ion-to-oxygen vector and the surface normal direction.[90] As expected, a uniform angular distribution is observed in the liquid phase. In the interfacial region, he found a diminished probability for a small angle value, indicating that the oxygen atom does not like to sit directly above the ion and point toward the vapor phase.

In an MD study of salt solutions, Jungwirth and Tobias examined the effects of surfaces on the orientation of hydrogen bonds between various ions and water molecules.[43] They found as the anion changes from F^-, Cl^-, Br^-, to I^-, there is a dramatic shift in the angular distribution function. For the F^- ion, the water−anion hydrogen bonds mostly point toward the bulk region, based on the computed $\cos(\theta)$ of −1. This finding is consistent with the picture that the surface is free of F^- ion, such that the anion−water hydrogen bonds come from the surface water molecules. For the larger halide anions such as Br^- or I^- in the interfacial region, the water−anion hydrogen bonds show a marked preference for being parallel to the interface. This behavior suggests that the interface cannot be depleted of ions. These results clearly demonstrate that the orientations of the ions and water are influenced by the presence of the interface. The use of molecular simulation techniques enables us to directly probe the structural changes at a molecular level.

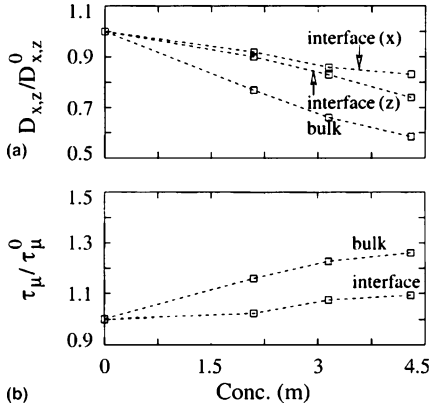

Figure 6. Relative changes of the (a) diffusion coefficients and (b) dipole orientational relaxation times of water molecules in the interfacial and bulk regions. (Adapted from ref 120.)

Jungwirth and co-workers have also carried out a series of studies using both MD and SFG techniques on the behavior of acids (i.e. HCl, HBr, and HI) and bases (NaOH) at the aqueous interfaces. A unified and consistent view of the structure of the air/solution interface of aqueous electrolytes containing monovalent inorganic ions was presented in the study. Their MD studies show that in salt solutions and bases the positively charged ions, such as alkali cations, are repelled from the interface, whereas the anions, such as halides or hydroxide, exhibit a varying surface propensity, correlated primarily with the ion polarizability and size. The behavior of acids is different due to the presence of hydronium cations at the air/solution interface. They found both cations and anions exhibit enhanced concentrations at the surface, and these acids reduce the surface tension of water. The results of the simulations are supported by surface selective nonlinear vibrational spectroscopy, which reveals among other things that the hydronium cations are present at the air/solution interface.

3.2. Dynamics at Interfaces

A large amount of interesting and important chemistry occurs at the interfaces between different phases, and there is a strong push for more attempts using nanotechnology to take advantage of unique interfacial properties. Diffusion is a fundamental property of chemical systems, and the ability to calculate it in a confined region is necessary for a complete understanding of the dynamics in an interfacial region. Recently, several MD studies have considered the dynamical properties of aqueous and aqueous electrolyte interfaces. These studies[120−122] focused on the diffusional and orientational relaxation of interfacial water molecules and ions and the effects of ion concentration on the dynamical behavior of such interfaces. Paul and Chandra reported that water molecules at interfaces are found to translate and rotate at a faster rate than bulk molecules because of the reduced density and lower number of hydrogen bonds in the interfacial region. They found a decrease in the interfacial width and an increase in the surface tension with increasing ion concentration. Figure 6 illustrates the relative changes of the

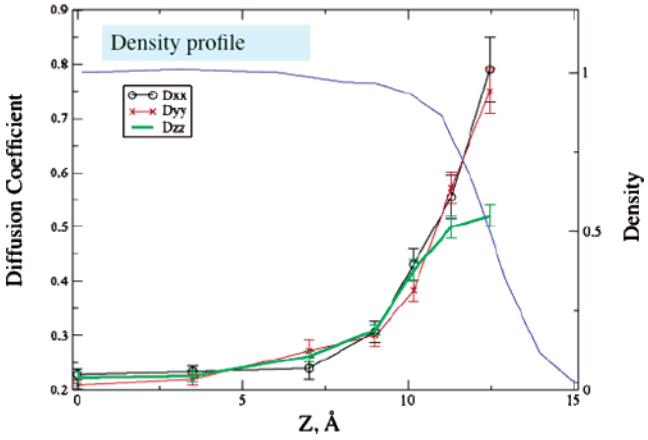

Figure 7. Plot of the diffusion coefficient in all three Cartesian coordinates for 3.5 Å regions extending from the bulk up to the interface. (Adapted from ref 121.)

diffusion coefficients and orientational relaxation times as a function of ion concentration. It can be concluded from these results that the dynamical properties of interfacial water molecules show a weaker change with ion concentration than those of bulk molecules.

Berne and co-workers have proposed a general methodology for calculating the self-diffusion tensor from molecular dynamics for a liquid with a liquid/gas or liquid/solid interface. They demonstrated that, far from the interface, the diffusion tensor is isotropic and the value of the diffusion coefficient agrees with that found in the bulk (Figure 7). As the layers approach the interface, the D_{zz} component of the diffusion coefficient at the interface is approximately two times the value in bulk water, while the components parallel to the interface are approximately three and half times the bulk value. Berne and co-workers concluded that the axial anisotropy in the diffusion is related to the structural asymmetry of the interface. Recently, Wick and Dang[122] carried out an MD study on a 2.2 M sodium chloride aqueous solution with a vapor/liquid interface using a methodology developed by Berne and co-workers. Wick and Dang found that the diffusion of all species was isotropic far away from the interface, but at different regions in the interface, the diffusion coefficients parallel to and perpendicular to the interface did not agree for water and the chloride ion. Specifically, the diffusion of interfacial water parallel to the interface was significantly higher than diffusion perpendicular to the interface. Chloride ions showed even larger anisotropicity in their diffusion coefficient at the interface. Their perpendicular diffusion is similar to the bulk value, but the parallel diffusion is much higher, corresponding to the region of highest chloride ion concentration. The origin for this behavior was found to be hydrogen bonds with water molecules, which are highly oriented perpendicular to the interface,[43] thus somewhat impeding chloride ion diffusion perpendicular to the interface. While sodium ion diffusion increased at the interface, its interfacial concentration was low in that region, and its diffusion was fairly isotropic throughout all regions. These results are illustrated in Figures 8 and 9.

3.3. Potential of Mean Force, Surface Tensions, and Surface Potentials

The behavior of solute molecules at liquid/vapor interfaces plays a critical role in diverse chemical and biological

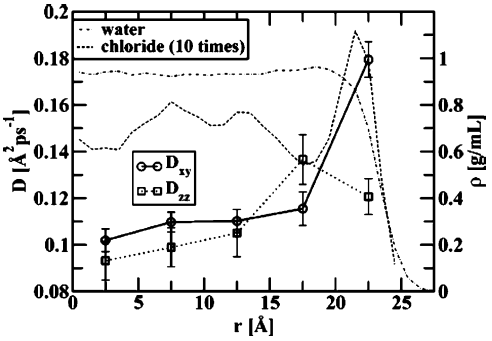

Figure 8. Chloride D_{xy} (circles and solid line) and D_{zz} (squares and dotted line) values along with the water specific density (dot−dashed line) and 10 times the chloride specific density (dashed line). (Adapted from ref 122.)

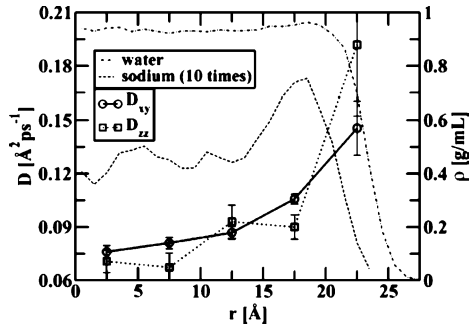

Figure 9. Sodium D_{xy} (circles and solid line) and D_{zz} (squares and dotted line) values along with the water specific density (dot−dashed line) and 10 times the sodium specific density (dashed line). (Adapted from ref 122.)

processes.[1−4,123] For example, the transport of trace gases or ions across aqueous interfaces is important in atmospheric processes such as molecular uptake.[124,125] The control of charge transfer processes across the liquid interfaces is relevant to liquid extraction and phase transfer catalysis,[5] and the adsorption and distribution of ions and amphiphilic solutes at aqueous interfaces impacts a wide range of phenomena from detergency to membrane integrity.[126,127]

To gain a complete understanding of the binding mechanisms and density distributions of ions near liquid interfaces, knowledge of the free energy associated with the chemical process is essential. Free energy dictates the chemical equilibrium and is considered to be one of the most important thermodynamic quantities. To this end, computer simulations provide a useful and practical approach for determining the free energy changes. Many computational techniques have been developed to determine the absolute solvation free energy in liquids. These approaches including free energy perturbation, thermodynamic integration, and the particle insertion method.[128−136] In general, free energy is difficult to determine for systems such as liquids that have many minima in the energy landscape separated by energy barriers. If care is taken to adequately sample the important region of phase spaces, these methods are shown to give reasonable estimates of the free energy difference between two states.

The free energy calculation is more complicated for the process at aqueous surfaces because the solvation free energy will depend on the location of the solute relative to the interface. Several approaches have been successfully applied to study the transport free energy of solute across various liquid interfaces.[42,89,137−141] Using an umbrella sampling technique with overlapping windows, Wilson and Pohorille were able to obtain the free energy profiles of Na^+, F^-, and

Cl^- ions as a function of their distance to the interface.[89] The free energies of ions are found to depend on their valence, and the free energy increases monotonically from the bulk to the interfacial region. Their study indicates that less energy is required to transport an anion across the interface than a cation. In addition, their study showed no evidence that the surface population of either the cation or anion is appreciable as the ions approach the interface.

Benjamin and co-workers also contributed a great deal to our understanding of solvation at liquid interfaces. They carried out a series of MD simulations to study the transfer of free energy of ions and organic solutes across the aqueous interface.[90,139] They found a positive adsorption free energy for ions, indicating a tendency for negative adsorption of ions at the interface. In all the above studies, effective pair potentials are employed in which polarization effects were not explicitly considered.

Using MD techniques and polarizable potential models, Dang and co-workers carried out an extensive study to investigate the transport of a wide range of ions across liquid/vapor interfaces. The transport mechanism is governed by the free energy profile or potential of mean-force (pmf).[42,45,98,115,142] To evaluate the free energies associated with the transfer of an ion across the interface, a constrained MD approach was used. To obtain a good approximation, the reaction coordinate for ion transfer can be considered to be the ion position along the interfacial normal direction (generally chosen to be the *z*-direction). The Helmholtz free energy difference, $\Delta F(z_s)$, between a state where the ion is located at z_s, $F(z_s)$, and a reference state where the ion is located at z_0, F_0, is simply

$$\Delta F(z_s) = F(z_s) - F_0 = -\int_{z_0}^{z_s} \langle f_z(z_s') \rangle \, dz_s' \qquad (2)$$

where $f_z(z_s')$ is the *z*-component of the total force exerted on the center of mass of the solute at a given *z*-position, z_s', averaged over the canonical ensemble. In general, F_0 was chosen as the free energy of the system with the solute located in the bulk liquid region. During the simulation, the *z*-coordinate of the solute was reset to its original value after each step and the average force acting on the solute was evaluated. The average forces are subsequently integrated to yield the free energy profile.

Depicted in Figure 10 are the computed free energy profiles of iodide anion binding to the liquid/vapor interface of water at 300 K from the work of Dang and Chang.[42] In this study, both polarizable and nonpolarizable potential models were used in the calculations of the solvent-averaged mean force and the corresponding pmf for moving I^- from bulk water through the interface into the vapor phase. These authors showed that both polarizable and nonpolarizable potential models yielded similar cluster and bulk-phase properties. However, it is evident from Figure 10 that the two models give qualitatively different results for the free energy profile at the interface. With the use of the polarizable potential models, they found that the ion could approach within two molecular layers of the Gibbs diving surface (GDS) from the liquid side without a significant change in the free energy. The computed free energy starts to decrease as the ion further approaches the GDS and exhibits a minimum near the GDS with a well depth of −1.5 kcal/mol. This minimum in the free energy profile indicates the stability of the surface state of the polarizable iodide ion at the interface. Beyond the GDS, the free energy begins to increase monotonically into the vapor-phase region because of the unfavorable ion−solvent interactions. Because the PMF is directly related to the probability of ions, the minimum in the PMF near the GDS indicates a surface enrichment of I^- ion, which agrees with the findings of Tobias and co-workers.[43] On the other hand, when the nonpolarizable interaction models are employed, the free energy profile is fairly flat in the bulk liquid region, which is similar to that predicted by the polarizable models. However, as the ion approaches the GDS, the free energy shows a substantial increase well into the vapor phase without a minimum near the GDS. This results shows that a nonpolarizable simulation predicts no surface stability as I^- anion crosses the liquid/vapor interface of water, in contrast to the predication obtained when polarizable potentials are used. The qualitative difference may be explained on the following physical basis: when a highly polarizable anion is near the liquid/vapor interface of polarizable water, because of the anisotropic solvation, the dipole moments of the anions and the local water molecules around the anion are increased. Consequently, an enhancement in the ion−dipole induction energies between the anion and water is obtained, leading to surface enrichment of the anion. This effect cannot be accounted for when the nonpolarizable model is used. This result demonstrates the importance of explicit treatment of the many-body polarization effect in molecular simulations.

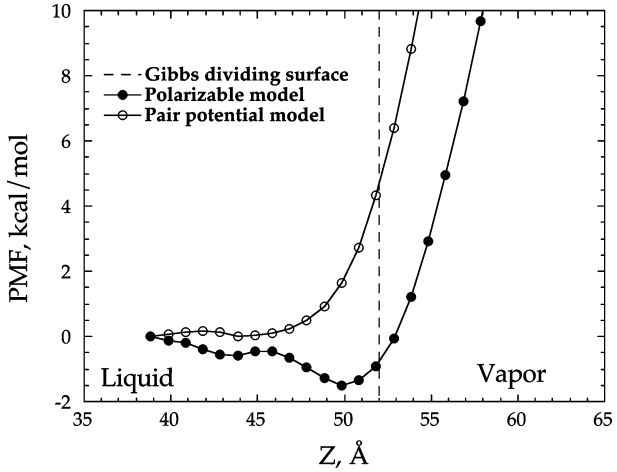

Figure 10. Computed free energy profiles for iodide ion binding to the liquid/vapor interface of water at 300 K: (solid circles) polarizable model; (open circles) nonpolarizable model. (Adapted from ref 42.)

Dang also carried out extensive MD simulations to investigate the molecular transport mechanisms of I^-, Br^-, Cl^-, and Na^+ ions across the liquid/vapor interface of water.[45,98] He evaluated the pmf of each ion and found that free energy profiles depend critically on the ion types. The larger I^- and Br^- anions are found to bind more strongly to the liquid/vapor interface, as indicated by the minimum near the GDS in the transfer free energy profiles, while the smaller anion Cl^- does not show such a minimum. This result, which is shown in Figure 11, is in good agreement with simulation work by Jungwirth and Tobias on the ion density distribution along the surface direction across the liquid/vapor interface.[43] Their computed density profiles for I^- and Br^- anions exhibited maxima near the GDS, whereas the density profile of Cl^- was quite flat. The computed pmf for Na^+ is very different from those of anions. As Na^+ approaches the GDS from the liquid side within two molecular layers, the free energy increases significantly and monotonically into the

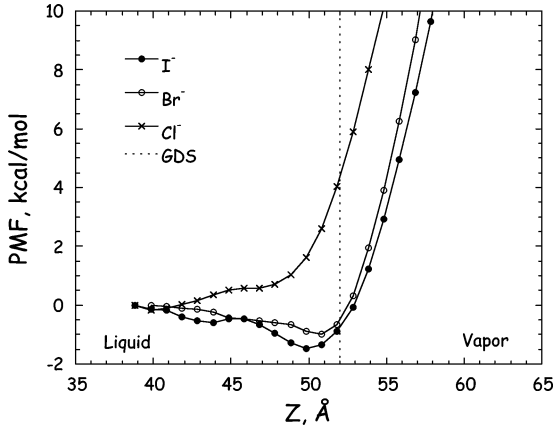

Figure 11. Computed free energy profiles for iodide, bromide, and chloride ions binding to the liquid/vapor interface of water at 300 K. (Adapted from ref 45.)

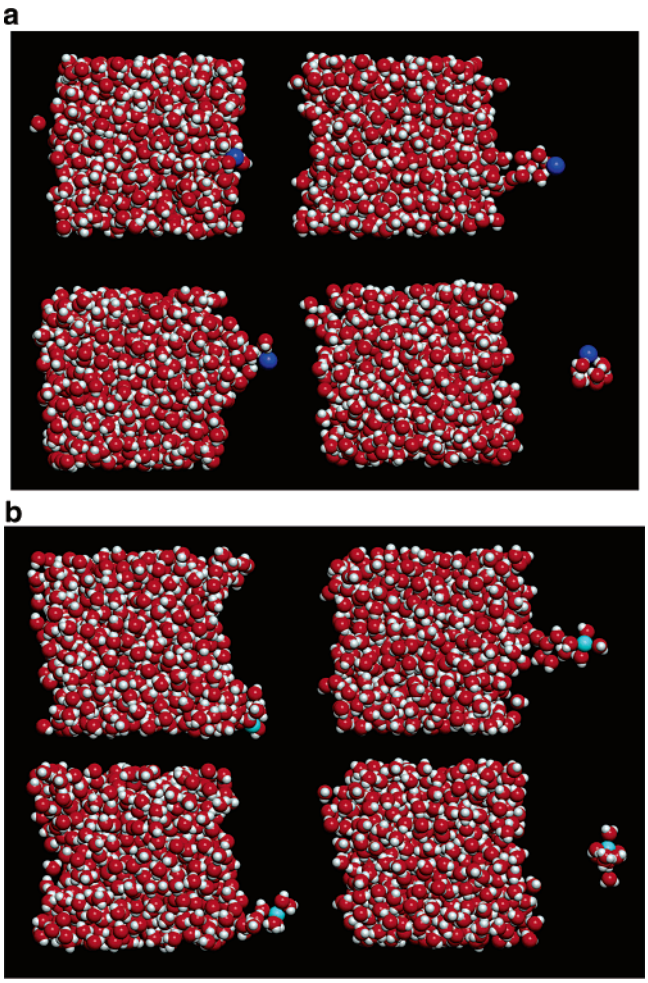

Figure 12. Snapshots taken from MD simulations using mean force approaches showing the Br^- and Na^+ ions leaving the liquid/vapor interface of water. (Adapted from ref 45.)

vapor phase. This is partly because of the small polarizability of Na^+ ion and partly because of the strong Na^+−water interaction. To understand the molecular mechanisms associated with ion transfer, Dang examined the local structures between the solvated ion and water along the free energy path. Depicted in Figure 12 are snapshots taken from MD simulations of Br^- (Figure 12a) and Na^+ (Figure 12b) ions at different locations as they cross the liquid/vapor interface. As clearly shown in Figure 12, both Br^- and Na^+ ions carried hydration shells as they moved from bulk into the vapor

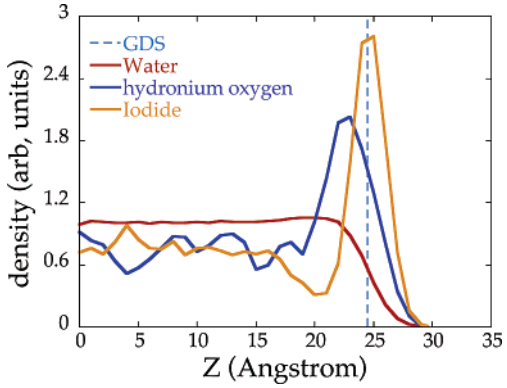

Figure 13. Computed density profiles of 2.2 M HI at the liquid/vapor interface of water.

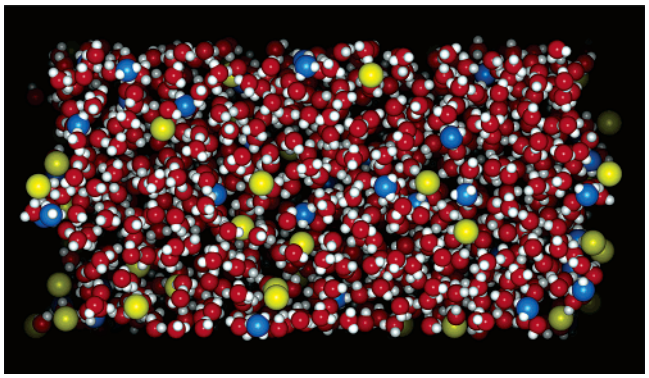

Figure 14. Snapshot of the distribution of 2.2 M HI at the liquid/vapor interface of water.

phase. The reason for the difference is that the solvation shell is much more tightly held by Na^+ ion as compared to the loosely held Br^-/water clusters. The difference in the Na^+-(H_2O) tightly packed shell and the $Br^-(H_2O)$ loosely packed shell is due to the stronger Na^+-H_2O interaction.

In addition to the above simulations, Dang has also carried out simulations to characterize the solvation properties of hydronium iodide (HI) salt at the water liquid/vapor interface and to compare these properties to those of the corresponding NaI salt/water interface. In Figure 13, the density profiles for water center-of-mass, $O_{H_3O^+}$, and I^- ions obtained from an MD simulation are presented.[42,98] Upon examining these density profiles as well as the MD simulation snapshots from Figure 14, the following three observations can be made. First, a significant number of iodide anions that formed a well-defined maximum are present near the dividing surface. The H_3O^+ molecules, on the other hand, are found near the interface as well as at the interface.[98] Second, this result differs from the results of NaI salt at the water liquid/vapor interface, in which the width of the electric double layer is smaller. This result is supported by the earlier studies by Dang on the pmf for the transport mechanism of an ion (Na^+ and H_3O^+) across the water liquid/vapor interface. As shown in Figure 15, the computed H_3O^+ pmf indicates that H_3O^+ is found closer to the dividing surface than the Na^+ ion and the computed free energy for H_3O^+ is lower (about 6 kcal/mol) at the dividing surface. Third, it is interesting to point out that the hydration energies and net charge of these ions are nearly identical; therefore, the different behavior of these ions at the aqueous interface can be attributed to differences in the shape, charge distribution, and polarizability of the H_3O^+ (Na^+) ion used in our classical simulations.

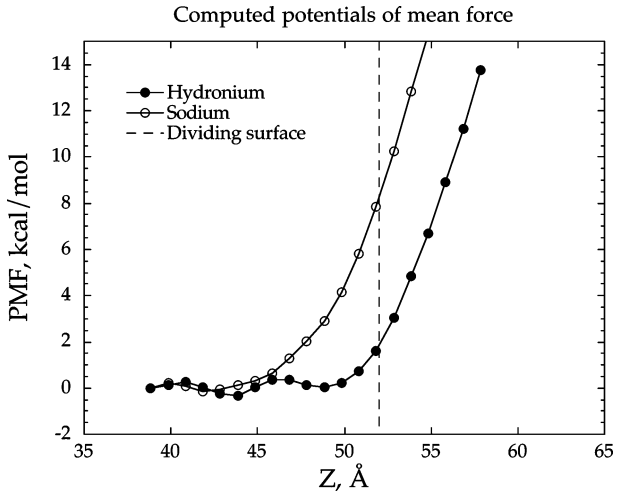

Figure 15. Computed free energy profiles for the hydronium and sodium ions binding to the liquid/vapor interface of water at 300 K. (Adapted from refs 45 and 98.)

The mechanism of proton transport in liquid water is quantum mechanical in nature; therefore, the classical polarizable model for H_3O^+ (i.e., fixed charge) may not accurately capture the $H_3O^+-H_2O$ interaction. It is well-known that the anomalous diffusion mechanism of H_3O^+ in water will strongly influence the results, and this mechanism is also known to have non-negligible quantum effects. An accurate study of the proton transport mechanism requires quantum statistical treatment of the hydrogen motion in liquid water. Thus, extension of this study to include quantum effects and comparison of the results to the results presented in this paper would be a worthwhile next step. It remains to be seen whether the mechanism of proton transport will have a substantial significant effect on the distribution of H_3O^+ at the interface. Because of its quantum nature, however, the characteristics of the hydrated proton in water remain a challenge. In summary, the hydronium ion study[98] may also contribute to the understanding of ion-induced nucleation of water vapor, which is thought to be of importance in many atmospheric processes. Dang's result is similar to the conclusion drawn by Voth and co-workers[103] in which the hydrated proton was found to exhibit a marked preference for the water liquid/vapor interface. In their multistate empirical valence bond approach, Voth and co-workers allowed for the explicit proton transfer between the hydronium ion and water, which may cause the discrepancy between these two studies. It will be worthwhile to investigate the effect of proton transfer on the solvation free energy profiles of the hydronium ion across the liquid/vapor interface. Using SHG techniques, Saykally and co-workers obtained the adsorption free energy for several ions at the liquid/vapor interface.[93,105,109,143] These authors examined the SHG response to the charge-transfer-to-solvent resonance as a function of the ion concentration. By fitting the normalized SHG intensities to the Langmuir isotherms, they were able to extract the Gibbs free energy of adsorption. They found negative free energies of SCN^-, I^-, and N_3^- ions, indicating these ions can be surface active.

Another problem of great interest is the effective interaction of the hydroxyl radical with water because of the role of the hydroxyl radical as a major oxidant in many biological, environmental, and man-made aqueous media. The uptake of hydroxyl radicals on aqueous surfaces is particularly important for atmospheric chemistry, as many atmospherically relevant reactions occur in or on aqueous atmospheric aerosols, cloud droplets, and thin water films on solid surfaces.[144] Understanding the uptake process as well as knowing whether the hydroxyl radical has a larger propensity for surface or bulk solvation is essential for elucidating the mechanisms of heterogeneous reactions taking place in the atmosphere. Roeselova et al.[145] assessed the equilibrium solvation behavior of the hydroxyl radical by computing a free energy profile for its transfer across the air/water interface. The resulting free energy profile is shown in Figure 16. The calculated value of the free energy of solvation agrees well with the experimental value, indicating that MD simulations with empirical potentials can provide very useful insights into processes involving radicals at the air/water interface. Future work will look at how the presence of ions influences the hydroxyl radical. The future work will include calculations of free energy profiles of hydroxyl radical for NaCl, NaBr, and NaI solutions to compare it with pure water.

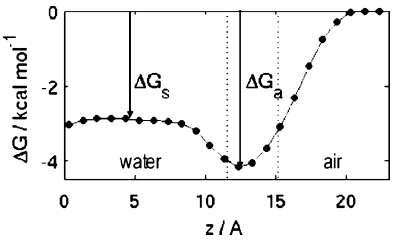

Figure 16. Free energy profile for transfer of a hydroxyl radical across the air/water interface. The interfacial region is indicated by the dotted lines. ΔG_s denotes the free energy of bulk solvation, and ΔG_a denotes the free energy of adsorption on the water surface. (Adapted from ref 145.)

Because of its importance in many atmospheric and environmental processes, the behavior of the nitrate ion in solution and at the water interface has recently been studied.[102] In particular, the manner in which water molecules solvate the nitrate ion is relevant to problems in chemical and physical processes such as chemical reactions at the interface. Jungwirth and co-worker have investigated this problem using classical and *ab initio* MD techniques.[102] They followed the trajectories of the nitrate ion at the interface and were able to conclude that the nitrate ion prefers to be at the interface rather than in the bulk as shown in Figure 17. Dang and co-workers[146] have also studied this problem using a different approach. They calculated the free energy profile for the transfer of a nitrate ion across the air/water interface. They found that the nitrate ion crossed the water interface with no free energy minimum as illustrated in Figure 18. Further research is underway to reconcile this difference.

Surface tension is one of the most important properties of liquid surfaces. This value of surface tension can be readily measured by many experimental techniques, and interpreting the behavior of surface tension contributes a great deal to our understanding of the interfacial phenomena of solutions. It is well-known that adding solutes changes the surface tension of water. In general, simple salts and bases increase the surface tension of water, while simple inorganic acids decrease the surface tension.[27,147] For example, experimental measurements have revealed that as the concentration of sodium halide increases, the surface tension of the aqueous solutions also increases. The only exception to this general rule is known as the Jones−Ray effect. At very dilute concentrations, an initial decrease and subsequently a minimum were observed in the surface tension of electrolyte

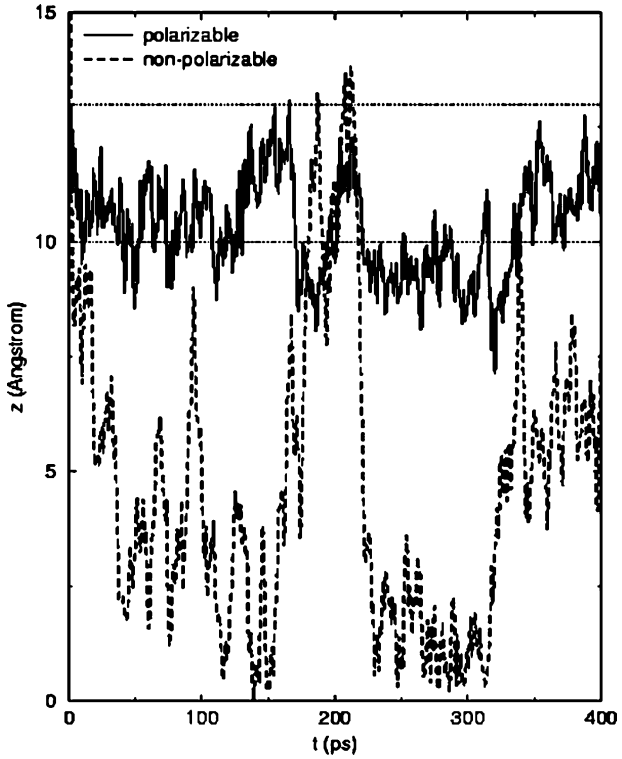

Figure 17. Distance of the nitrate anion from the slab center during 0.4 ns from a classical molecular dynamics simulation. (Adapted from ref 102.)

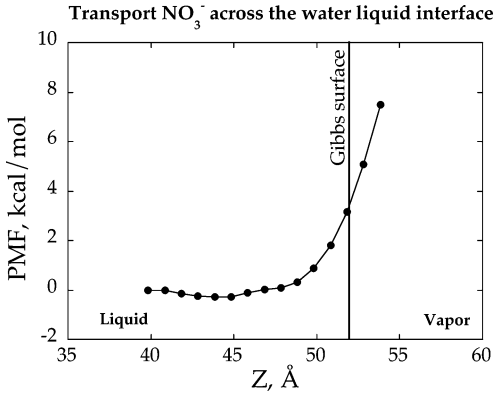

Figure 18. Computed pmf for the nitrate ion binding to the liquid/vapor interface of water.

solutions at about 1 mM concentrations.[25,93]

The observation of surface tension incremental changes with added electrolyte along with the Gibbs adsorption equation predicts a negative adsorption of ions at the interface. Additionally, the surface tensions of electrolyte solutions show marked ion-specific effects known as a Hofmeister series.[148,149] In a homologous series of monovalent anions with a common cation (and *vice versa*), the increase in surface tension is larger for more strongly hydrated (or smaller) ions. Many theoretical approaches have been developed to understand this ion-specific effect.[150−153] Molecular simulations have also been carried out to evaluate surface tensions of various liquid interfaces.[18,154−157] These studies in part try to reproduce the experimental data and in part try to develop a molecular understanding of the surface tension.

It is straightforward to evaluate the liquid/vapor interfacial tension from MD simulations.[157] From the elements of the internal pressure tensor as the difference between the normal and tangential components, the surface tension is simply[158,159]

$$\gamma = (L_z/2)((p_{xx} + p_{yy}/2) - p_{zz}) \tag{3a}$$

Here, the *z*-axis is chosen to be the surface normal direction. $P_{\alpha\alpha}$ ($\alpha = x, y,$ or z) is the $\alpha\alpha$ element of the pressure tensor, and L_z is the linear dimension of the simulation cell in the *z*-direction. The element of the pressure tensor can be calculated according to the virial equation as

$$p_\alpha\beta = \frac{1}{V}\left(\sum_{i=1}^{N} m_i v_{i\alpha} v_{i\beta} + \frac{1}{2}\sum_{i'=1}^{N'}\sum_{j'=1}^{N'} F_{i'j'\alpha} r_{ij\beta}\right) \tag{3b}$$

where N and N' are the numbers of molecules and atoms in the system, respectively. V is the total volume, m_i is the mass of molecule i, and $v_{i\alpha}$ is the center-of-mass velocity of molecule i, respectively. In eq 3b, $F_{i'j'\alpha}$ is the α component of the force exerted on atom i' of molecule i due to the atom j' of molecule j, and $r_{ij\beta}$ is the β component of the vector connecting the center-of-mass of molecules i and j.

In a recent MD simulation, Jungwirth and Tobias evaluated surface tensions of a series of 1.2 M sodium halide solutions.[43] Polarizable interaction potentials were employed in their study. Although the computed surface tensions do not exactly reproduce the experimental values, their values do show a slight incremental difference with respect to those for pure water, which agrees with experimental observations. Moreover, the simulation correctly predicts the trend of the surface tension increase, that is, NaF > NaCl > NaBr > NaI. However, when the ion distribution was analyzed along the interfacial normal direction, some unexpected results were observed, as noted in a previous section. For a NaF solution, they predicted that the Na^+ and F^- ions would be repelled from the interface, which is consistent with the Gibbs equation. For larger halide solutions, NaCl, NaBr, and NaI, the simulations showed that while Na^+ ions are repelled from the interface, Cl^-, Br^-, and I^- anions exhibit increasing concentration enhancement near the interface. Despite the positive adsorption of these anions, the surface tensions of these salt solutions still show an increase when compared to that of pure water. This may be explained by the nonmonotonic distribution of ions along the interface direction. Their findings suggest that an increase in surface tension does not exclude the possibility of positive solute adsorption near the interfaces.

Radke and co-workers performed MD simulations to evaluate the surface tensions of NaF, NaCl, and NaBr aqueous solutions as a function of salt concentration.[154,160] They adopted pairwise additive potentials to describe the molecular interactions. In their study, they closely reproduced the experimental surface tensions at lower concentrations. They also observed a negative adsorption of all the ions at the interface. As the concentration increased, they observed a buildup of ion densities near the interface, eventually leading to a positive adsorption at high enough salt concentrations. Corresponding to the onset of the positive ion adsorption, the surface tension shows a maximum and then a noticeable decline, which differs from the experimental trend. It is also worth noting that the cation and anion density profiles closely mimic each other in their simulations. This behavior was not observed in other studies mentioned earlier. Further investigation is required to define the polarization effect on ion solvation at the liquid/vapor interfaces. Dang[161] also investigated the change in surface tension of acidic

aqueous solutions of HI as a function of concentration. He found that the surface tension decreases with increasing concentration, which is in qualitative agreement with the experimental results.

Surface potential, χ, is another property that has been widely used to determine the molecular structure at the liquid interfaces. This quantity, which is the electrostatic potential difference at the boundary between the liquid and vapor phases, is sensitive to the molecular orientation and composition of the interfaces. Both experiments and simulations have shown that water molecules exhibit preferred orientations near the liquid/vapor interface as a result of changing molecular interaction patterns. Such orientational ordering is expected to induce electric double layers and cause an electrostatic potential difference across the liquid/vapor interfaces.[162] The surface potential can be useful in understanding the solvation and transfer of ions in electrolyte solutions. Despite extensive experimental studies, surface potential values are still difficult to obtain.[163,164] In the literature, the reported values of χ range from -1.10 to 0.50 V for the pure water/vapor interface.[87,165−168] Scattered experimental results also exist for aqueous and nonaqueous electrolyte solutions.[169,170]

Most of the previous theoretical developments on surface potential were based on a continuum model and lacked molecular details.[38,165,171] Molecular simulations have made considerable progress in providing a molecular description of the equilibrium properties at the liquid interfaces of water and aqueous solutions. In particular, many of the simulation efforts have focused on computing the surface potential.[118,172−178] Similar to the experimental situation, the computed values of surface potential are found to vary widely because of the sensitivity of the potential model and computational methods.[179,180]

It is well-known that, because of the induction effect, the dipole moment of water in the liquid phase is different from that in the gas phase.[51] The incorporation of polarizability in molecular models provides a way to systematically account for the enhanced dipole moment of a water monomer in condensed phase environments compared to an isolated gas-phase monomer. Because the surface potential depends critically on the molecular orientation at the interface, an understanding of the polarization effect on molecular orientation at the vapor/liquid interfaces is important. Berkowitz and co-workers addressed this effect by carrying out MD simulations using polarizable and nonpolarizable water models.[181] They concluded that polarization effects are of secondary importance in predicting the orientation structure at the neat water liquid/vapor interface.

Two main approaches, atomic and molecular, have been reported in the literature for computing surface potentials from molecular simulations.[172,173] The atomic approach accounts for the distributions of the partial charge and induced dipole moment associated with each interaction site of the particular model potentials. The molecular dipole approach considers the electrostatic potential caused by the total dipole moment associated with each molecule in the simulation. Interestingly, these two methods generally have yielded inconsistent results for the same set of simulation data. In the following discussion, both methods are briefly described.

The atomic approach examines the effects of the distributions of atomic partial charges and induced dipole moments on the electrostatic potential difference across the liquid/vapor interface. For simulations using nonpolarizable (Coulombic) potential models, the only contribution to the surface potential comes from the atomic partial charge distribution. By computing $Q_+(z)$ ($Q_-(z)$), the sums of the atomic partial charges for atoms located above (below) coordinate z in the interface normal direction, the mean electric field at location z, $E(z)$, can be estimated as

$$E(z) = (\langle Q_-(z) - Q_+(z)\rangle/2\epsilon_0 A) \tag{4}$$

Here, $\langle ... \rangle$ indicates a configurational average, A is the interface area, and ϵ is the permittivity of the free space. Because water molecules do not possess any net charge, the contribution to $E(z)$ comes only from water molecules that have hydrogen and oxygen atoms extended both above and below coordinate z. By integrating the mean electric field along the surface normal direction, the electric potential difference across the interface, $\Delta\phi_q(z)$, can be determined by

$$\Delta\phi_q(z) = \phi_q(z) - \phi_q(z_0) = -\int_{z_0}^{z} E(z')\, dz' \tag{5}$$

In this equation, z_0 denotes a reference point in the charge-free (vapor) region. If polarizable potential models are employed in MD simulations, there is an additional contribution to the electrostatic potential from the induced dipole moment associated with each interaction site as a result of the atomic polarizability. The distribution of the atomic induced dipole moments along the interface normal direction, $\langle \rho_\mu^{ind}(z)\rangle$, can be evaluated as the average sum of the normal (z) component of the atomic induced dipole moments in the liquid slabs of 0.1 Å thickness parallel to the interface. Once the induced dipole moment distribution is determined, the electrostatic potential difference across the interface, $\Delta\phi_\mu^{ind}(z)$, can be estimated using the following equation.

$$\Delta\phi_\mu^{ind}(z) - \Delta\phi_\mu^{ind}(z_0) = \frac{1}{\epsilon_0}\int_{z_0}^{z}\langle \rho_\mu^{ind}(z')\rangle\, dz' \tag{6}$$

By adding the contributions from the partial charges and atomic induced dipole moments, the total surface potential can be obtained.

The molecular dipole approach calculates the surface potential that results from the alignment of the total dipole moments of water molecules. As mentioned above, water molecules exhibit preferred orientation near the interface and induce surface potential across the interface. To compute this electrostatic potential change, the distribution profile of the total dipole moments of water molecules is determined as a function of the molecular z-coordinate. By calculating the normal component of the total molecular dipole moments per unit volume centered at location z', $\rho_\mu^{tot}(z')$, using liquid slabs of 0.1 Å thickness parallel to the interface, we can evaluate the relative surface potential change between coordinates z and z_0 as

$$\Delta\phi_\mu^{tot}(z) - \Delta\phi_\mu^{tot}(z_0) = \frac{1}{\epsilon_0}\int_{z_0}^{z}\langle \rho_\mu^{tot}(z')\rangle\, dz' \tag{7}$$

Past studies[172,173] obtained different results for the surface potentials across the liquid/vapor interface from the use of the atomic approach and the molecular dipole approach. It has been argued that these discrepancies come from the fact that the molecular approach neglects the higher order moment

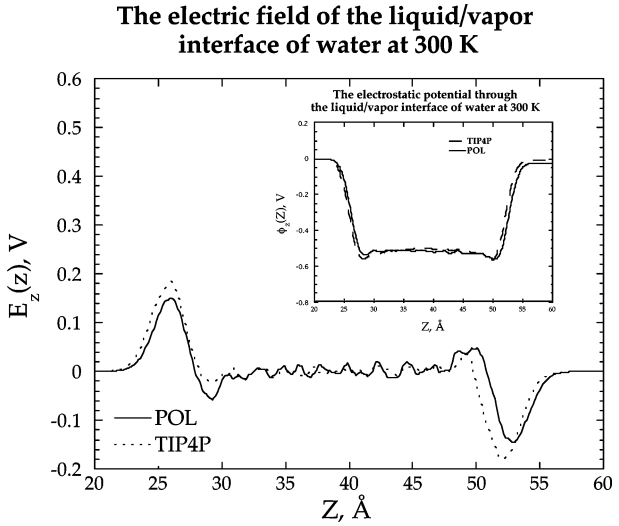

Figure 19. Electric field across the water liquid/vapor interface at 300 K as a function of the *z*-coordinate based on the atomic approach. The inset is the atomic-based electric potential change across the water liquid/vapor interface at 300 K. (Adapted from ref 42.)

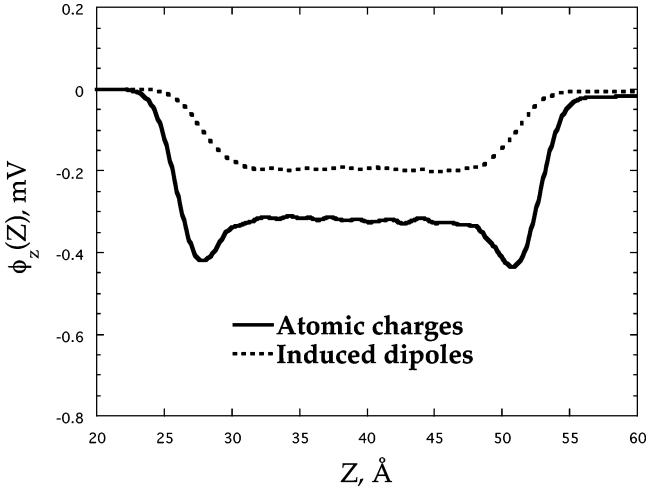

Figure 20. Contributions to the electrostatic potentials from the partial atomic charge density and from the induced dipole moment distribution. (Adapted from ref 42.)

contributions to the surface potential. When the quadrupole term is included in the surface potential calculations, the two methods yield similar results.[172,173]

Wilson et al.[172] conducted an MD simulation to investigate the surface potential of pure water based on the atomic approach. With the use of the TIP4P water potential model,[182] they found a surface potential of $-(110 \pm 50)$ mV. Using a molecular dipole approach, Matsumoto and Kataoka found a positive surface potential of 0.16 V at the water/air interface.[173] Dang and Chang[42] carried out MD simulations to examine the electric potential across the water/vapor interface based on the atomic and molecular dipole approaches. Shown in Figure 19 are the data for the computed electric field due to the partial atomic charge distributions across the water/vapor interfaces as a function of the *z*-coordinate at 298 K. As clearly seen in Figure 19, the electric fields in the vapor phases and in the *bulk* liquid region are close to zero, as expected. The small oscillations observed between both interfaces are the results of truncation effects. The results of Dang and Chang[42] are almost identical to the results reported recently by Sokhand and Tildesley using the SPC/E water model and Ewald summation techniques.[118] Because the simulation system[42] is arranged in a way such that the liquid slab of water is sandwiched between two vapor phases, the electric field is observed to be antisymmetric about the center-of-mass of the bulk liquid. It was found that the electric field first increased and went through a maximum when the interface was first approached from the lower vapor side. As the water layers were penetrated, the electric field changed sign and gradually converged to zero. Pratt and co-workers[172] observed similar effects in their earlier studies.

To check the effect of the explicit polarizability on the interfacial electrostatic properties, the simulation results of the electric fields using both polarizable and nonpolarizable water potential models are displayed in Figure 19.[42] Except that the nonpolarizable model predicts slightly larger electric fields near the interfaces, these two models yield quantitatively and qualitatively very similar results. This observation suggests that the explicit inclusion of the polarization energy component into the water potential model has a negligible effect on the electrostatic properties at the liquid/vapor interface. The inset shows the calculated electric potentials across the liquid/vapor interface of water based on the atomic approach. Clearly, the simulations with polarizable and nonpolarizable potential models predict essentially the same features and values of the surface potential. If the interface is approached from the vapor phase, the electric potential is observed to decrease into the bulk liquid regions and shows a shallow minimum just inside the interfacial region before it levels off. This result indicates that the polarization effects are of secondary importance in predicting the electrostatic properties across the liquid/vapor interface. This conclusion is similar to the earlier study by Berkowitz and co-workers.[181] The surface potential is evaluated to be -500 ± 10 mV, which lies within the experimental data of χ in the range of -1.1 to 0.5 V. The wide spread of experimental estimates[87] of χ resulted from the various approximations used to infer χ, which has only been indirectly determined from experiments.

As discussed earlier, if the polarizable potential models are used in the simulations, there will be contributions to the electrostatic potentials from the partial atomic charge density and from the induced dipole moment distribution. Depicted in Figure 20 are the separate contributions to the electrostatic potential change across the interface, $\phi(z)$, from these two atomic properties. As clearly demonstrated in this plot, the atomic charge contribution to the electric potential, $\phi_q(z)$, is the dominant component and shows similar features to those of the total electrostatic potential. On the other hand, the electric potential change resulting from the induced dipoles, $\phi_\mu^{\mathrm{ind}}(z)$, is found to decrease monotonically from the vapor phase to the bulk liquid region and is shown to be of lesser importance. The surface potential resulting from the alignment of the total dipole moments of water molecules was also evaluated using the molecular dipole approach The computed electric potential change across the liquid/vapor interface showed strikingly different behavior than that obtained using the atomic approach. The computed surface potential was found to be $+400$ mV, which is greatly different from the -500 mV value estimated using the atomic approach.[87] The large discrepancy may be because the molecular dipole approach neglects the higher order moment contribution to the surface potential as suggested by Pratt and co-workers.[180]

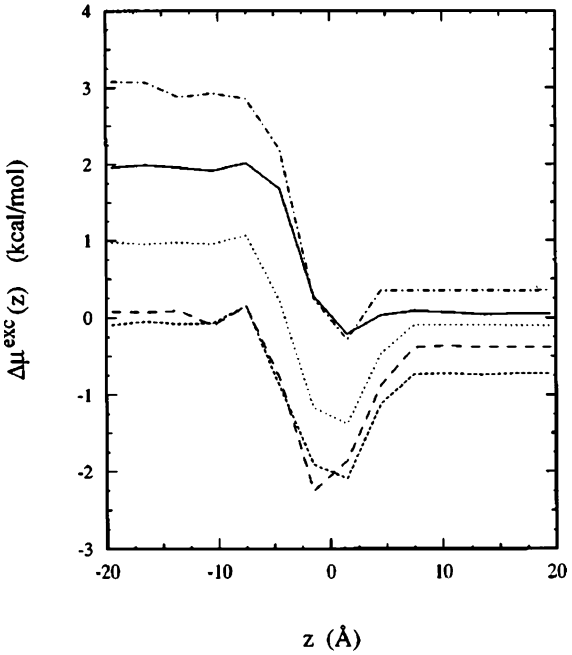

Figure 21. Excess chemical potential of CH_4 (solid line), CH_3F (short dashed line), CH_2F_2 (long dashed line), CHF_3 (dotted line), and CF_4 (dot−dashed line) at 310 K along the *z*-direction perpendicular to the water/hexane interface (located at $z = 0$). Water is on the left and hexane is on the right side. (Adapted from ref 136.)

4. Progress in Liquid/Liquid Interface Simulations

4.1. Transport of Organic Solutes

Computer simulation techniques provide a useful and practical approach to the study of solute transfer processes across liquid/liquid interfaces. With the use of MD techniques, Marrink and Berendsen carried out simulations to study the transport of water molecules through phospholipid/water systems.[137] Through the use of a Lennard-Jones liquid/liquid interface and MD methods, Hayoun and co-workers[47] described solute transfer as an activated process that reflects the changes in the degree of solvation by the two solvents. Pohorille and Wilson[136] investigated the excess chemical potentials of a series of small solutes across the water/membrane and water/hexane interfaces. Their results, which are presented in Figure 21, showed that the shape of the free energy profiles depends on the magnitude of the dipole moments of the solute molecules. Chang and Dang examined the solvation structures, free energy profile, and transport mechanism associated with the transfer of a small organic solute—a single chloroform—across the CCl_4/H_2O liquid/liquid interface.[183] The free energy change between two different solute locations in the free energy profiles represents the reversible work necessary to bring the solute from one position to the other. The region through which the free energy undergoes changes extends over roughly 10 Å, which yields an estimate of the interfacial width. In both cases, the organic solute exhibits free energy stability in the bulk CCl_4 relative to that in the bulk H_2O phase. The free energy difference is 6.5 kcal/mol for the transfer of a chloroform molecule. The decrease in free energy in the nonaqueous phase is consistent with the fact that $CHCl_3$ is more soluble in CCl_4 than in H_2O. The free energy profile exhibits a monotonic decrease from the aqueous phase into the organic phase. Interestingly, the dipolar solute, chloroform, is not surface active, as indicated by the fact that no interfacial minimum is observed in the free energy profile.

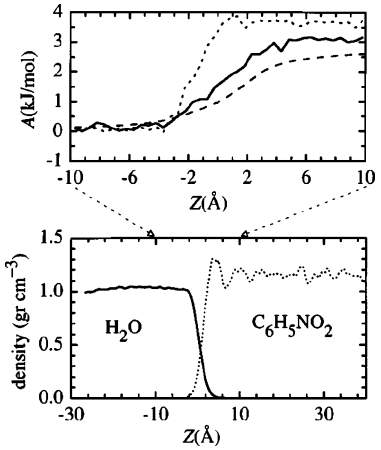

Figure 22. (Top panel) The pmf for the transfer of TMA across the water/nitrobenzene interface: (solid line) calculated using the solute location distribution function; (dotted line) calculated using the integral of the average force on the ion; (dashed line) results of a continuum electrostatic model. (Bottom panel) Density profiles of water and nitrobenzene showing the liquid/liquid interface region where the solute is located. (Adapted from ref 184.)

4.2. Transport of Ions

Interest in computer simulation of ion transport has intensified since Benjamin's pioneering work on the mechanism and dynamics of transferring a single chlorine ion across a water/1,2-dichloroethane interface.[48] Due to the approximations made on the electrostatic free energy calculation, Benjamin suggested that, because of the presence of a free energy minimum (∼5 kcal/mol) at the liquid/liquid interface, ion transfer into the aqueous phase is an activated process. Schweighfer and Benjamin[184] recently studied transport of TMA (tetramethyl ammonium) from water to the nitrobenzene liquid/liquid interface and found no barrier when the system was fully equilibrated as indicated in Figure 22. In a paper describing their MD study on the structural and energetic characteristics of ion-assisted transfer between water and chloroform, Wippf and co-workers[185] reported that the cesium ion diffuses spontaneously from the interface to water and displays apparently no free energy minimum. Recently, Fernandes and co-workers[186] reported a series of MD simulations on ion transfer processes from water to organic solvents. Their computed ion transfer free energies are in reasonable agreement with the experimental data, and no minima were observed at the liquid/liquid interface. Dang[187] carried out several studies on the mechanism for transporting ions across a chlorinated hydrocarbon/water liquid/liquid interface. That included the simulations of Cs^+ and Cl^- across the water/carbon tetrachloride liquid/liquid interface. He found that the free energies exhibited a monotonic increase from the aqueous phase into the organic phase and underwent major changes as the ion began to cross the interface. No barrier was found at the liquid/liquid interface. During the transfer process, the coordination number for the ions as a function of the *z*-axis normal to the interface was monitored. As the ions moved across the interface, the first hydration shell of the ion began to be reduced as shown in Figure 23. The characteristic features shown in this figure are clearly similar to the computed free energy profile. Thus, an ion transfer mechanism that involves changes in the hydration shell of the ion has been demon-

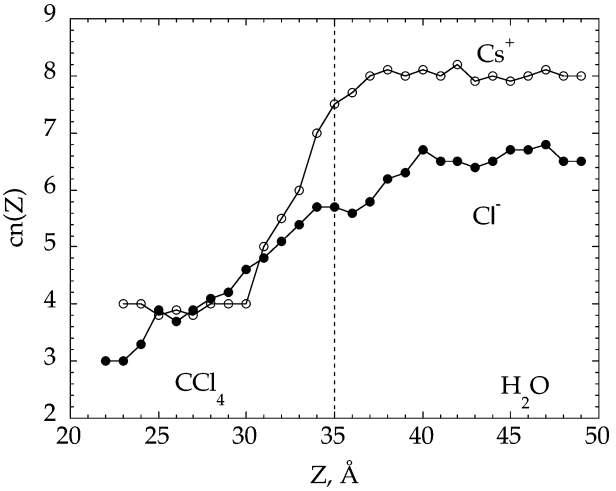

Figure 23. Computed hydration numbers of the ions as a function of *z*-axis normal to the interface. (Adapted from ref 187.)

strated. This finding is in excellent agreement with a recent experimental study by Osakai and co-workers,[188] who measured the Gibbs free energy of ion transfer between water and nitrobenzene for various ions. They also measured the water content in nitrobenzene and found a fraction of water associated with the ion in the nitrobenzene liquid phase. For example, the coordination number of Na^+ is approximately six in water. The coordination number decreased to approximately four when the ion was transferred to nitrobenzene.

Dang also reported the pmf for transferring an iodide anion across the water/dichloromethane liquid/liquid interface.[49] Upon carefully examining the free energy profile, he found it exhibits a more complicated transfer process as compared to those for other ions such as Cl^- or Cs^+. He found that there was no well-defined barrier at the liquid/liquid interface as was found in the case of the liquid/vapor interface; however, the computed pmf showed a stabilization free energy of -1.0 kcal/mol as the I^- ion approached the liquid/liquid interface. This result indicates that there is a significantly greater probability to find an I^- ion near the interface than in the bulk liquid. The computed free energy undergoes major changes as the ion begins to cross the interface. The change in free energy is positive because the I^- was shedding the water molecules as it crossed the interface. The estimated free energy of transfer is 12 ± 2 kcal/mol. There is an experimental measurement of 6 kcal/mol for transferring a single ion I^- from the liquid water to the liquid dichloromethane at room temperature. However, the comparison with this experimental data may not be appropriate because our simulated data have indicated that the ion drags some water molecules along with it across the interface.

5. Conclusion

The study of ion solvation at liquid/vapor and liquid/liquid interfaces is an important topic of active research motivated by their applications in a wide area of chemistry and biology. In this paper, we review the contribution of MD simulations to a variety of chemical and physical processes in solutions and at interfaces. Our main emphasis is on recent advances in the understanding of ion solvation, molecular association, and molecular solvation at liquid interfaces. The species discussed range from monovalent ions to molecular ions such as hydronium and nitrate ions. It is found that small ions are repelled from the liquid/vapor interfaces, which is consistent with the Gibbs adsorption equations. On the other hand, both experiments and molecular simulations have revealed that certain ions, especially the larger polarizable ions, exhibited surface affinity. However, the complete molecular interpretation of this behavior is still elusive and requires further investigation.

We also noted that surface enhancements for ions are more pronounced when polarizable potential models are used. The MD simulations demonstrate the importance of properly treating the polarization effect in molecular interactions. Explicitly incorporating polarization effects into a potential model is still an evolving science. We believe that simulations of ion solvation at the interface with explicitly included polarization effects are important, because at the interface the water dipole moments are significantly different from bulk values (i.e., $\mu \sim 2.0$ D at the interface and $\mu \sim 2.7$ D in the bulk liquid). Therefore, the interactions between solute and solvent at the interface will affect the computed results (i.e., free energy of solvation or spectroscopic properties of solute solvation at the interface).

6. Acknowledgments

This work was performed at Pacific Northwest National Laboratory (PNNL) under the auspices of the Division of Chemical Sciences, Office of Basic Energy Sciences, U.S. Department of Energy. PNNL is operated by Battelle. The DOE Division of Chemical Sciences and the Scientific Computing Staff, Office of Energy Research, at the National Energy Research Supercomputer Center (Berkeley, California) provided computer resources that supported this research.

7. References

(1) Franks, F.; Mathias, S. E. *Biophysics of Water*; Wiley: Chichester, 1982.
(2) Grossfield, A.; Ren, P. Y.; Ponder, J. W. *J. Am. Chem. Soc.* **2003**, *125*, 15671.
(3) Paul, S.; Chandra, A. *Chem. Phys. Lett.* **2004**, *400*, 515.
(4) Benjamin, I. *Chem. Rev.* **1996**, *96*, 1449.
(5) Starks, C. M.; Liotta, C. L.; Halpern, M. *Phase Transfer Catalysis*; Chapman & Hall: New York, 1994.
(6) Veziriglu, T. N. *Environmental Problems and Solutions: Greenhouse Effect, Acid Rain, Pollution*; Hemisphere: New York, 1990.
(7) Zhuang, X.; Miranda, P. B.; Kim, D.; Shen, Y. R. *Phys. Rev. B* **1999**, *59*, 12632.
(8) Miranda, P. B.; Shen, Y. R. *J. Phys. Chem. B* **1999**, *103*, 3292.
(9) Eisenthal, K. B. *Chem. Rev.* **1996**, *96*, 1343.
(10) Richmond, G. L. *Chem. Rev.* **2002**, *102*, 2693.
(11) Als-Nielsen, J.; Jacquemain, D.; Kjaer, K.; Leveiller, F.; Lahav, M.; Leiserowitz, L. *Phys. Rep.* **1994**, *246*, 252.
(12) Bowers, J.; Zarbakhsh, A.; Webster, J. R. P.; Hutchings, L. R.; Richards, R. W. *Langmuir* **2001**, *17*, 140.
(13) Shen, Y. R. *The Principles of Nonlinear Optics*; John Wiley & Sons: New York, 1984.
(14) Raduge, C.; Pflumio, V.; Shen, Y. R. *Chem. Phys. Lett.* **1997**, *274*, 140.
(15) Shultz, M. J.; Baldelli, S.; Schnitzer, C.; Simonelli, D. *J. Phys. Chem. B* **2002**, *106*, 5313.
(16) Baldelli, S.; Schnitzer, C.; Shultz, M. J. *J. Chem. Phys.* **1998**, *108*, 9817.
(17) Allen, M. P.; Tildesley, D. J. *Computer Simulation of Liquids*; Oxford University: Oxford, 1987.
(18) Alejandre, J.; Tildesley, D. J.; Chapela, G. A. *J. Chem. Phys.* **1995**, *102*, 4574.
(19) Lee, J. K.; Barker, J. A.; Pound, G. M. *J. Chem. Phys.* **1974**, *60*, 1976.
(20) Linse, P. *J. Chem. Phys.* **1987**, *86*, 4177.
(21) Gao, J.; Jorgensen, W. L. *J. Phys. Chem.* **1988**, *92*, 5813.
(22) Benjamin, I. *J. Chem. Phys.* **1992**, *97*, 1432.
(23) Chang, T.-M.; Dang, L. X. *J. Chem. Phys.* **1996**, *104*, 6772.
(24) Heydweiller, A. *Ann. Phys.* **1910**, *4*, 145.
(25) Jones, G.; Ray, W. A. *J. Am. Chem. Soc.* **1937**, *59*, 187.

(26) Dole, M.; Swartout, J. A. *J. Am. Chem. Soc.* **1940**, *62*, 3039.
(27) Weissenborn, P. K.; Pugh, R. J. *J. Colloid Interface Sci.* **1996**, *184*, 550.
(28) Matubayasi, N.; Tsunetomo, K.; Sato, I.; Akizuki, R.; Morishita, T.; Matuzawa, A.; Natsukari, Y. *J. Colloid Interface Sci.* **2001**, *243*, 444.
(29) Matubayasi, N.; Matsuo, H.; Yamamoto, K.; Yamaguchi, S.; Matuzawa, A. *J. Colloid Interface Sci.* **1999**, *209*, 398.
(30) Gibbs, J. W. *The Collected Works of J. Willard Gibbs*; Longmans: New York, 1928.
(31) Adamson, A. W.; Gast, A. P. *Physical Chemistry of Surfaces*, 6th ed.; Wiley-Interscience: New York, 1997.
(32) Langmuir, I. *J. Am. Chem. Soc.* **1917**, *39*, 1848.
(33) Wagner, C. *Phys. Z.* **1924**, *25*, 474.
(34) Onsager, L.; Samaras, N. N. T. *J. Chem. Phys.* **1934**, *2*, 528.
(35) Dean, D. S.; Horgan, R. R. *Phys. Rev. E* **2004**, *69*, 061603.
(36) Hsin, W. L.; Sheng, Y. J.; Lin, S. Y.; Tsao, H. K. *Phys. Rev. E* **2004**, *69*, 031605.
(37) Levin, Y. *J. Chem. Phys.* **2000**, *113*, 9722.
(38) Markin, V. S.; Volkov, A. G. *J. Phys. Chem. B* **2002**, *106*, 11810.
(39) Knipping, E. M.; Lakin, M. J.; Foser, K. L.; Jungwirth, P.; Tobias, D. J.; Gerber, R. B.; Dabdub, D.; Finlayson-Pitts, B. J. *Science* **2000**, *288*, 301.
(40) Hu, J. H.; Shi, Q.; Davidovits, P.; Worsnop, D. R.; Zahniser, M. S.; Kolb, C. E. *J. Phys. Chem.* **1995**, *99*, 8768.
(41) Laskin, A.; Gaspar, D. J.; Wang, W.; Hunt, S. W.; Cowin, J. P.; Colson, S. D.; Finlayson-Pitts, B. J. *Science* **2003**, *301*, 340.
(42) Dang, L. X.; Chang, T.-M. *J. Phys. Chem. B* **2002**, *106*, 235.
(43) Jungwirth, P.; Tobias, D. J. *J. Phys. Chem. B* **2001**, *105*, 10468.
(44) Liu, D.; Ma, G.; Levering, L. M.; Allen, H. C. *J. Phys. Chem. B* **2004**, *108*, 2252.
(45) Dang, L. X. *J. Phys. Chem. B* **2002**, *106*, 10388.
(46) Raymond, E. A.; Richmond, G. L. *J. Phys. Chem. B* **2004**, *108*, 5051.
(47) Hayoun, M.; Meyer, M.; Turq, P. *J. Phys. Chem.* **1994**, *98*, 6626.
(48) Benjamin, I. *Science* **1993**, *261*, 1558.
(49) Dang, L. X. *J. Phys. Chem. B* **2001**, *105*, 804.
(50) Gregory, J. K.; Clary, D. C.; Liu, K.; Brown, M. G.; Saykally, R. J. *Science* **1997**, *275*, 814.
(51) Dang, L. X.; Chang, T.-M. *J. Chem. Phys.* **1997**, *106*, 8149.
(52) Dang, L. X. *J. Phys. Chem.* **1998**, *102*, 620.
(53) Silvestrelli, P. L.; Parrinello, M. *Phys. Rev. Lett.* **1999**, *82*, 3308.
(54) Badyal, Y. S.; Saboungi, M. L.; Price, D. L.; Shastri, S. D.; Haeffner, D. R.; Soper, A. K. *J. Chem. Phys.* **2000**, *1112*, 9206.
(55) Batista, E. R.; S., X. S.; Jonsson, H. *J. Chem. Phys.* **1998**, *109*, 4546.
(56) Coulson, C.; Eisenberg, D. *Proc. R. Soc. London, Ser. A* **1966**, *291*, 445.
(57) Shepard, A. C.; Beers, Y.; Klien, G. P.; Rothman, L. S. *J. Chem. Phys.* **1973**, *59*, 2254.
(58) Dymanus, A.; Verhoeven, J. *J. Chem. Phys.* **1970**, *52*, 3222.
(59) Kuo, I.-F. W.; Mundy, C. J. *Science* **2004**, *303*, 658.
(60) Perera, L.; Berkowitz, M. L. *J. Chem. Phys.* **1991**, *95*, 1954.
(61) Perera, L.; Berkowitz, M. L. *Z. Phys. D* **1992**, *26*, 166.
(62) Perera, L.; Berkowitz, M. L. *J. Chem. Phys.* **1992**, *96*, 8288.
(63) Sremaniak, L. S.; Perera, L.; Berkowitz, M. L. *Chem. Phys. Lett.* **1994**, *218*, 377.
(64) Perera, L.; Berkowitz, M. L. *J. Chem. Phys.* **1994**, *100*, 3085.
(65) Dang, L. X.; Rice, J. E.; Caldwell, J.; Kollman, P. A. *J. Am. Chem. Soc.* **1991**, *113*, 2481.
(66) Dang, L. X. *J. Chem. Phys.* **1992**, *96*, 6970.
(67) Hiraoka, K.; Mizuse, S.; Yamabe, S. *J. Phys. Chem. A* **1988**, *92*, 3943.
(68) Markovich, G.; Pollack, S.; Giniger, R.; Sheshnovsky, O. *Z. Phys. D* **1993**, *26*, 98.
(69) Arshadi, M.; Yamdagni, R.; Kebarle, P. *J. Phys. Chem.* **1970**, *74*, 1475.
(70) Hertel, I. V.; Huglin, C.; Nitsch, C.; Schulz, C. P. *Phys. Rev. Lett.* **1991**, *67*, 1767.
(71) Choi, J. H.; Kuwata, K. T.; Cao, Y. B.; Okumura, M. *J. Phys. Chem. A* **1988**, *102*, 503.
(72) Ayotte, P.; Bailey, C. G.; Weddle, G. H.; Johnson, M. A. *J. Phys. Chem. A* **1998**, *102*, 3067.
(73) Ayotte, P.; Bailey, C. G.; Weddle, G. H.; Johnson, M. A. *J. Phys. Chem. A* **1999**, *103*, 443.
(74) Cabarcos, O. M.; Weinheimer, C. J.; Lisy, J. M.; Xantheas, S. S. *J. Chem. Phys.* **1999**, *110*, 5.
(75) Jorgensen, W. L.; Severance, D. L. *J. Chem. Phys.* **1993**, *99*, 4233.
(76) Dang, L. X.; Smith, D. E. *J. Chem. Phys.* **1993**, *99*, 6950.
(77) Stuart, S. J.; Berne, B. J. *J. Phys. Chem.* **1996**, *100*, 11934.
(78) Stuart, S. J.; Berne, B. J. *J. Phys. Chem. A* **1999**, *103*, 10300.
(79) Ramaniah, L. M.; Bernasconi, M.; Parrinello, M. *J. Chem. Phys.* **1998**, *109*, 6839.
(80) Yoo, S.; Lei, Y. A.; Zeng, X. C. *J. Chem. Phys.* **2003**, *119*, 6083.
(81) Herce, D. H.; Perera, L.; Darden, T. A.; Sagui, C. *J. Chem. Phys.* **2005**, *122*, 024513.
(82) Hagberg, D.; Brdarski, S.; Karlstrom, G. *J. Phys. Chem. B* **2005**, *109*, 4111.
(83) Combariza, J. E.; Kestner, N. R.; Jortner, J. *Chem. Phys. Lett.* **1993**, *203*, 423.
(84) Caldwell, J. W.; Kollman, P. A. *J. Phys. Chem.* **1992**, *96*, 8249.
(85) Xantheas, S. S.; Dang, L. X. *J. Phys. Chem.* **1996**, *100*, 3989.
(86) Xantheas, S. S. *J. Phys. Chem.* **1996**, *100*, 9703.
(87) Randles, J. E. B. *Chem. Phys. Liq.* **1977**, *7*, 107.
(88) Wilson, M. A.; Pohorille, A.; Pratt, L. R. *Chem. Phys.* **1989**, *129*, 209.
(89) Wilson, M. A.; Pohorille, A. *J. Chem. Phys.* **1991**, *95*, 6005.
(90) Benjamin, I. *J. Chem. Phys.* **1991**, *95*, 3698.
(91) Gopalakrishnan, S.; Jungwirth, P.; Tobias, D. J.; Allen, H. C. *J. Phys. Chem. B* **2005**, *109*, 8861.
(92) Ghosal, S.; Hemminger, J. C.; Bluhm, H.; Mun, B. S.; Hebenstreit, E. L. D.; Ketteler, G.; Ogletree, D. F.; Requejo, F. G.; Salmeron, M. *Science* **2005**, *307*, 563.
(93) Petersen, P. B.; Saykally, R. J. *Chem. Phys. Lett.* **2004**, *397*, 51.
(94) Wennerstrom, H. *Curr. Opin. Colloid Interface Sci.* **2004**, *9*, 163.
(95) Netz, R. *Curr. Opin. Colloid Interface Sci.* **2004**, *9*, 192.
(96) Jungwirth, P.; Tobias, D. J. *J. Phys. Chem. B* **2000**, *104*, 7702.
(97) Garrett, B. C. *Science* **2004**, *303*, 5661.
(98) Dang, L. X. *J. Chem. Phys.* **2003**, *119*, 6351.
(99) Jungwirth, P.; Tobias, D. J. *J. Phys. Chem. B* **2002**, *106*, 6361.
(100) Mucha, M.; Frigato, T.; Levering, L. M.; Allen, H. C.; Tobias, D. J.; Dang, L. X.; Jungwirth, P. *J. Phys. Chem. B* **2005**, *109*, 7617.
(101) Brown, E. C.; Mucha, M.; Jungwirth, P.; Tobias, D. J. *J. Phys. Chem. B* **2005**, *109*, 7934.
(102) Salvador, P.; Curtis, J. E.; Tobias, D. J.; Jungwirth, P. *Phys. Chem. Chem. Phys.* **2003**, *5*, 3752.
(103) Petersen, M. K.; Iyengar, S. S.; F., D. T. J.; Voth, G. A. *J. Phys. Chem. B* **2004**, *108*, 14804.
(104) Agmon, N. *Chem. Phys. Lett.* **1995**, *244*, 456.
(105) Petersen, P. B.; Saykally, R. J. *J. Phys. Chem. B* **2005**, *109*, 7976.
(106) Mukamel, S. *Principles of Nonlinear Optical Spectrocopy*; Oxford University Press: Oxford, 1995.
(107) Shen, Y. R. *Annu. Rev. Phys. Chem.* **1989**, *40*, 327.
(108) Vidal, F.; Tadjeddine, A. *Rep. Prog. Phys.* **2005**, *68*, 1095.
(109) Petersen, P. B.; Saykally, R. J.; Mucha, M.; Jungwirth, P. *J. Phys. Chem. B* **2005**, *109*, 10915.
(110) Hribar, B.; Southall, N. T.; Vlachy, V.; Dill, K. A. *J. Am. Chem. Soc.* **2002**, *124*, 12301.
(111) Dill, K. A.; Truskett, T. M.; Vlachy, V.; Hribar-Lee, B. *Annu. Rev. Biophys. Biomol. Struct.* **2005**, *34*, 173.
(112) Frediani, L.; Mennucci, B.; Cammi, R. *J. Phys. Chem. B* **2004**, *108*, 13796.
(113) Du, Q.; Superfine, R.; Freysz, E.; Shen, Y. R. *Phys. Rev. Lett.* **1993**, *70*, 2313.
(114) Wilson, K. R.; Schaller, R. D.; Co, D. T.; Saykally, R. J.; Rude, B. S.; Catalano, T.; Bozek, J. D. *J. Chem. Phys.* **2002**, *117*, 7738.
(115) Dang, L. X. *J. Phys. Chem. A* **2004**, *108*, 9014.
(116) Patel, S.; Brooks, C. L., III. *J. Chem. Phys.* **2005**, *122*, 024508.
(117) Richmond, G. L. *Annu. Rev. Phys. Chem.* **2001**, *52*, 357.
(118) Sokhan, V. P.; Tildesley, D. J. *Mol. Phys.* **1997**, *92*, 625.
(119) Schnitzer, C.; Baldelli, S.; Shultz, M. J. *J. Phys. Chem. B* **2000**, *104*, 585.
(120) Paul, S.; Chandra, A. *Chem. Phys. Lett.* **2003**, *373*, 87.
(121) Liu, P. L.; Harder, E.; Berne, B. J. *J. Phys. Chem. B* **2004**, *108*, 6595.
(122) Wick, C. D.; Dang, L. X. *J. Phys. Chem. B* **2005**, *109*, 15574.
(123) Marrink, S. J.; Berkowitz, M. L.; Berendsen, H. J. C. *Langmuir* **1993**, *9*, 3122.
(124) Finlayson-Pitts, B. J.; Pitts, J. N., Jr. *Atmospheric Chemistry: Fundamentals and Experimental Techniques*; Wiley: New York, 1986.
(125) Finlayson-Pitts, B. J. *Chem. Rev.* **2003**, *103*, 4801.
(126) McCoy, M. *Chem. Eng. News* **2003**, *81*, 15.
(127) Groot, R. D.; Rabone, K. L. *Biophys. J.* **2001**, *81*, 725.
(128) Singh, U. C.; Brown, F. K.; Bash, P. A.; Kollman, P. A. *J. Am. Chem. Soc.* **1987**, *109*, 1607.
(129) Warshel, A.; Parson, W. W. *Annu. Rev. Phys. Chem.* **1991**, *42*, 279.
(130) Straatsma, T. P.; McCammon, J. A. *Annu. Rev. Phys. Chem.* **1992**, *43*, 407.
(131) Straatsma, T. P.; Berendsen, H. J. C. *J. Chem. Phys.* **1988**, *89*, 5876.
(132) Mitchell, M. J.; McCammon, J. A. *J. Comput. Chem.* **1991**, *12*, 271.
(133) Guillot, B.; Guissani, Y. *J. Chem. Phys.* **1993**, *99*, 8075.
(134) Widom, B. *J. Phys. Chem.* **1982**, *86*, 869.
(135) Sok, R. M.; Berendsen, H. J. C.; Vangunsteren, W. F. *J. Chem. Phys.* **1992**, *96*, 4699.
(136) Pohorille, A.; Wilson, M. A. *J. Chem. Phys.* **1996**, *104*, 3760.
(137) Marrink, S. J.; Berendsen, H. J. C. *J. Phys. Chem.* **1994**, *98*, 4155.
(138) Chipot, C.; Wilson, M. A.; Pohorille, A. *J. Phys. Chem. B* **1997**, *101*, 782.

(139) Pohorille, A.; Benjamin, I. *J. Chem. Phys.* **1991**, *94*, 5599.
(140) Chang, T.-M.; Dang, L. X. *J. Chem. Phys.* **1998**, *108*, 818.
(141) Benjamin, I. *Acc. Chem. Res.* **1995**, *28*, 233.
(142) Dang, L. X.; Garrett, B. C. *Chem. Phys. Lett.* **2004**, *385*, 309.
(143) Petersen, P. B.; Johnson, J. C.; Knutsen, K. P.; Saykally, R. J. *Chem. Phys. Lett.* **2004**, *397*, 46.
(144) Finlayson-Pitts, B. J.; Pitts, J. N. *Chemistry of the Upper and Lower Atmosphere: Theory, Experiments, and Applications*; Academic Press: San Diego, CA, 2000.
(145) Roeselova, M.; Vieceli, J.; Dang, L. X.; Garrett, B. C.; Tobias, D. J. *J. Am. Chem. Soc.* **2004**, *126*, 16308.
(146) Dang, L. X.; Chang, T. M.; Roselova, M.; Garrett, B. C.; Tobias, D. J. *J. Chem. Phys.*, submitted.
(147) Weissenborn, P. K.; Pugh, R. J. *Langmuir* **1995**, *11*, 1422.
(148) Collins, K. D.; Washabaugh, M. W. *Q. Rev. Biophys.* **1985**, *18*, 323.
(149) Bostrom, M.; Kunz, W.; Ninham, B. W. *Langmuir* **2005**, *21*, 2619.
(150) Katsov, K.; Weeks, J. D. *J. Phys. Chem. B* **2002**, *106*, 8429.
(151) Kunz, W.; Lo Norstro, P.; Ninham, B. W. *Curr. Opin. Colloid Interface Sci.* **2004**, *9*, 1.
(152) Kunz, W.; Belloni, L.; Bernard, O.; Ninham, B. W. *J. Phys. Chem. B* **2004**, *108*, 2398.
(153) Manciu, M.; Ruckenstein, E. *Adv. Colloid Interface Sci.* **2003**, *105*, 63.
(154) Bhatt, D.; Newman, J.; Radke, C. J. *J. Phys. Chem. B* **2004**, *108*, 9077.
(155) Aguado, A.; Wilson, M.; Madden, P. A. *J. Chem. Phys.* **2001**, *115*, 8603.
(156) Mecke, M.; Winkelmann, J.; Fischer, J. *J. Chem. Phys.* **1997**, *107*, 9264.
(157) Trokhymchuk, A.; Alejandre, J. *J. Chem. Phys.* **1999**, *111*, 8510.
(158) Kirkwood, J. G.; Buff, F. P. *J. Chem. Phys.* **1949**, *17*, 338.
(159) Rowlinson, J. R.; Widom, B. *Molecular Thory of Capillarity*; Oxford University Press: Oxford, 1989.
(160) Bhatt, D.; Chee, R.; Newman, J.; Radke, C. J. *Curr. Opin. Colloid Interface Sci.* **2004**, *9*, 145.
(161) Dang, L. X. Unpublished.
(162) Duncanhewitt, W. C. *Langmuir* **1991**, *7*, 1229.
(163) Krishtalik, L. I.; Alpatova, N. M.; Ovsyannikova, E. V. *J. Electroanal. Chem.* **1992**, *329*, 1.
(164) Paluch, M. *Adv. Colloid Interface Sci.* **2000**, *84*, 27.
(165) Parfenyuk, V. I. *Colloid. J.* **2002**, *64*, 651.
(166) Jarvis, N. L.; Scheiman, M. A. *J. Phys. Chem.* **1968**, *72*, 74.
(167) Farrell, J. R.; McTigue, P. *J. Electroanal. Chem.* **1982**, *37*, 1982.
(168) Eley, D. D.; Evans, M. G. *Trans. Faraday Soc.* **1938**, *34*, 1093.
(169) Ringeisen, B. R.; Muenter, A. H.; Nathanson, G. M. *J. Phys. Chem. B* **2002**, *106*, 4988.
(170) Chorny, I.; Benjamin, I.; Nathanson, G. M. *J. Phys. Chem.* **2004**, *108*, 995.
(171) Parfenyuk, V. I. *Colloid. J.* **2004**, *66*, 466.
(172) Wilson, M. A.; Pohorille, A.; Pratt, L. R. *J. Chem. Phys.* **1988**, *88*, 3281.
(173) Matsumoto, M.; Kataoka, Y. *J. Chem. Phys.* **1988**, *88*, 3233.
(174) Madden, W. G.; Gomer, R.; Mandell, M. J. *J. Phys. Chem.* **1977**, *81*, 2652.
(175) Zakharov, V. V.; Brodskaya, E. N.; Laaksonen, A. *J. Chem. Phys.* **1997**, *107*, 10675.
(176) Barraclough, C. G.; McTigue, P. T.; Ng, Y. L. *J. Electroanal. Chem.* **1992**, *329*, 9.
(177) Smondyrev, A. M.; Berkowitz, M. L. *Biophys. J.* **1999**, *76*, 2472.
(178) Warshavsky, V. B.; Bykov, T. V.; Zeng, X. C. *J. Chem. Phys.* **2001**, *114*, 504.
(179) Torrie, G. M.; Patey, G. N. *J. Phys. Chem.* **1993**, *97*, 12909.
(180) Pratt, L. R. *J. Phys. Chem.* **1992**, *96*, 25.
(181) Motakabbir, K. A.; Berkowitz, M. L. *Chem. Phys. Lett.* **1991**, *176*, 61.
(182) Jorgensen, W. L.; Chandrasekhar, J.; Madura, J. D.; Impey, R. W.; Klein, M. L. *J. Chem. Phys.* **1983**, *79*, 926.
(183) Chang, T. M.; Dang, L. X. *Chem. Phys. Lett.* **1996**, *263*, 39.
(184) Schweighofer, K.; Benjamin, I. *J. Phys. Chem. A* **1999**, *103*, 10274.
(185) Lauterbach, L.; Engler, E.; Muzet, N.; Troxler, L.; Wippf, G. *J. Phys. Chem. B* **1998**, *102*, 245.
(186) Fernandes, P.; Natalia, A.; Cordeiro, M.; Gomes, D. S. *J. Phys. Chem.* **2000**, *104*, 2278.
(187) Dang, L. X. *J. Phys. Chem. B* **1999**, *103*, 8195.
(188) Osakai, T.; Ogata, A.; Ebina, K. *J. Phys. Chem.* **1997**, *101*, 8341.

CR0403640